

Experimental investigation of tensile and bond properties of Carbon-FRCM composites for strengthening masonry elements

Francesca Giulia Carozzi ^{a, *}, Alessandro Bellini ^b, Tommaso D'Antino ^c,
Gianmarco de Felice ^d, Francesco Focacci ^e, Łukasz Hojdys ^f, Luca Laghi ^g, Emma Lanoye ^h,
Francesco Micelli ⁱ, Matteo Panizza ^j, Carlo Poggi ^a

^a Department of Architecture, Built Environment and Construction Engineering, Politecnico di Milano (PoliMi), Milan, Italy

^b CIRI Buildings and Construction, University of Bologna (UniBO), Bologna, Italy

^c Department of Civil Engineering, University of Patras (UPatras), Patras, Greece

^d Department of Engineering, Roma3 University (UniRM3), Rome, Italy

^e University eCampus (UnieCampus), Novedrate, Italy

^f Faculty of Civil Engineering, Cracow University of Technology (CUT), Cracow, Poland

^g Certimac c/o Enea Temaf (Certimac), Laboratorio di ricerca analisi e prove, Faenza, Italy

^h University Claude Bernard Lyon 1 (Unilyon), Laboratory of Composite Materials for Construction (LMC2), Lyon, France

ⁱ Department of Engineering for Innovation (UniLE), University of Salento, Lecce, Italy

^j Department of Civil, Architectural and Environmental Engineering, University of Padova (UniPD), Padua, Italy

Fabric Reinforced Cementitious Matrix (FRCM) materials are composed of a dry fiber grid embedded in an inorganic matrix, which may contain short fibers.

These materials are particularly well-suited for the reinforcement of masonry structures due to their high compatibility with the substrate, vapor permeability and durability against environmental agents.

The most important information needed for the characterization of these composite systems, for use as strengthening materials of masonry structures, are the tensile behaviour and the shear bond properties. A Round-Robin Test was organized by the RILEM Technical Committee 250-CSM and the Italian association Assocompositi in order to experimentally characterize different FRCM systems composed of PBO, carbon, glass, basalt, aramid and steel textiles embedded in cementitious or lime-based mortars. The systems were tested at different universities and research centers in Europe in order to investigate the influence of samples preparation, test set-up and instrumentation.

In this paper, the experimental tests performed on Carbon-FRCM systems are described and discussed. Important aspects are analyzed herein: differences in the testing procedure and instrumentation, influence of textile geometry and mechanical properties of the constituent materials, importance of specimen preparation and curing conditions. Moreover, a comparison between tensile and shear tests is reported in order to determine a reliable procedure towards the complete characterization of an FRCM material.

Keywords:

Fabric reinforced cementitious matrix (FRCM)

Textile reinforced mortar (TRM)

Masonry

Strengthening

Experimental investigation

Carbon fibers

1. Introduction

Fabric Reinforced Cementitious Matrix (FRCM) materials represent an innovative retrofitting system comprising a fiber textile embedded into an inorganic matrix. The reinforcement could be manufactured of different types of textiles (e.g. carbon, glass, basalt, aramid, PBO, steel) usually in the form of continuous yarns arranged in such a way to form grids with different

geometries. The textile could be unidirectional or bi-directional, usually nylon fibers are used as a supporting mesh. Steel material could be presented as steel cords or textile made of unidirectional steel cords kept in place by a glass fiber mesh, in this cases the composite is named Steel Reinforced Grout (SRG). The matrices are composed of cementitious or lime-based mortars, in some cases enriched with polymers (at low volume contents) or short fibers.

Composite materials are used both in new structures (e.g. for the production of thin-walled prefabricated elements) and for the retrofitting of masonry and concrete structures. FRCMs are a

* Corresponding author. Piazza Leonardo Da Vinci, 32, Milan, Italy.
E-mail address: francescagiulia.carozzi@polimi.it (F.G. Carozzi).

particular type of Textile Reinforced Mortar (TRM) that are specifically used for strengthening.

When applied to masonry substrates, they are preferable to Fiber Reinforced Polymer (FRP) strengthening systems due to their major compatibility with the substrate, reversibility, vapor permeability, better resistance to high temperatures, and durability against detrimental agents [1,2]. An overview of the use of FRCM systems can be found in Refs. [3–8].

Although a technical guide is provided by the American Concrete Institute [9], in Europe, guidelines and codes for characterization and design of FRCM systems are not available, the only document available concerns textile reinforced concrete [10]. The knowledge of the mechanical behaviour and bond properties of these materials is very important for their use as rehabilitation/strengthening systems. The characterization of these materials involves the analysis of the tensile and bond behaviour (with different substrates), thus standard tensile and bond tests are necessary.

Various set-ups for tensile tests on FRCM specimens have been developed [11–17]. The specimen preparation, dimension and shape, the clamping system and the load application may largely influence the resulting stress-strain behaviour.

Different specimen geometries have been proposed. The rectangular shape is the easiest to implement and produce. This shape is recommended also because the textile reinforces the total width of the specimen cross-section. A second possibility is the dumbbell [18], for which the specimen section was gradually increased at its ends and a perforated metal plate was placed at mid-thickness to ensure the load transmission. This solution involves the use of a vertical mold; it presents some difficulties in positioning the perforated plate but seems attractive because it overcomes the effects of the differential shrinkage between the sides of the plate. A third possibility [19] is the use of a bone-shaped specimen, which requires expensive moulds and particular care in implementation; moreover, many tests results showed failure close to specimen ends where the cross-section thickness is varied. To obtain failure at the mid-span of the sample a V-notched parallelepiped was used; this configuration allows good results in the analyses of the strength, but the imposed location of the first crack prevents measurement of the overall behaviour and limits the scope of the results [13]. Test set-ups and consequent failure modes are very important parameters because the stress distribution among filaments and yarns is influenced by the matrix cracking [20].

For externally bonded FRP materials the most common failure mode is the debonding of the composite strip with the detachment of a layer of substrate. The stress-transfer mechanism in FRCM materials, between the composite and the substrate and between the textile and the matrix, is influenced by different phenomena (e.g.: mechanical and adhesion properties, textile geometry, mortar granulometry). The failure modes could be different and influenced by geometrical and mechanical properties of the grid and the matrix. The most common failure mode is the debonding at the textile-to-matrix interface followed by slippage of the grid within the matrix [21–23].

The shear test set-up is based on the application of a direct tensile force to the reinforcement applied on one side (single-lap) [24–27], or on two opposite sides of the specimen (double-lap) [26–29]. In single-lap shear tests the grid free length can include dry yarns or can be impregnated with an organic or inorganic matrix, in order to guarantee a homogeneous stress distribution among yarns. Both single- and double-lap set-ups present some drawbacks. In particular, the former could be influenced by eccentricity (out-of-plane) phenomena and misalignment of the textile, which can influence the test results. In the latter, it is important to guarantee the homogeneous stress distribution at the two laps. Moreover, if one of the two bonded sides starts failing, the

system loses the symmetry and the alignment between the textile and the axis of the testing machine.

To investigate the mechanical properties of different FRCM systems, the RILEM Technical Committee 250-CSM “Composites for Sustainable Strengthening of Masonry” organized a Round Robin experimental campaign that involved 21 universities and research institutions and 11 companies. The main objectives of this campaign were the comparison between the performance and the mechanical properties of different FRCM materials, constituted of carbon, glass [30], basalt [31], aramid and PBO [32] and steel [33] textiles. The influence of the following parameters was considered: the textile geometry, textile and matrix mechanical and bond properties, test set-up, specimens preparation and curing procedure [34].

In this paper the extensive experimental campaign on FRCM systems including carbon fibers textile is described. Both tensile and bond properties are analyzed, the experimental test procedure and the main results are illustrated and the influence of the different experimental parameters is discussed.

2. Mechanical properties of FRCM components

The FRCM systems analyzed in this work are constituted of an inorganic matrix and a carbon fiber grid. Different systems were investigated. The matrices were lime- or cement-based and enriched with a low content of polymers. The textiles are characterized by different geometry, mass density, yarn treatment and mechanical properties. In the following, the different textiles are labeled as C_n, and the correspondent systems as C-FRCM_n. A total of six C-FRCM systems were analyzed, each system was investigated in two or three different laboratories.

In the following, the geometrical properties of the textiles involved are described (Fig. 1), all the textiles present a balanced bidirectional structure, the cross-section area of the yarns in the orthogonal directions are equal.

The “C₁” and “C₃” textiles are identical bidirectional open weaved fabrics with a high temperature resistant coating. The nominal spacing mid-yarn to mid-yarn is equal to 30 mm and the surface mass density is equal to 220 g/m².

The “C₂” balanced bidirectional textile has an equivalent thickness equal to 0.047 mm and a mass density of 170 g/m².

The carbon fiber “C₄” is a balanced grid with fiber yarns arranged in two orthogonal directions (Fig. 1c). The equivalent fiber thickness is 0.047 mm in both directions and the mass density is equal to 168 g/m². The yarns are uncoated.

The “C_{5a}” balanced bidirectional textile is made with yarns nominally spaced at 17.5 mm with an equivalent thickness equal to 0.048 mm and a mass density equal to 200 g/m². The “C_{5b}” bidirectional textile presents the same mechanical properties of textile C_{5a}, but with a different spacing mid-yarn to mid-yarn equal to 9.4 mm and an equivalent thickness equal to 0.061 mm.

The “C₆” textile is a balanced grid with a nominal spacing of 20 mm and an equivalent thickness equal to 0.047 mm in both directions, the mass density is equal to 170 g/m². The yarns are coated.

The coating used is applied only in the external part of the yarns and doesn't impregnate the internal filaments that are free to slip.

Tensile tests on the fibers non-impregnated by the mortar were performed on single yarns and on grid strips of width 40 and 50 mm in the warp direction. The tests performed at PoliMi and UPatras were performed on a single yarn, while the samples used at UniRM3 were composed of five yarns.

In Table 1, the mechanical properties of the textile and of the mortar are reported. It should be highlighted that the mortar used in the system C-FRCM₁ is composed of hydraulic lime without cement.

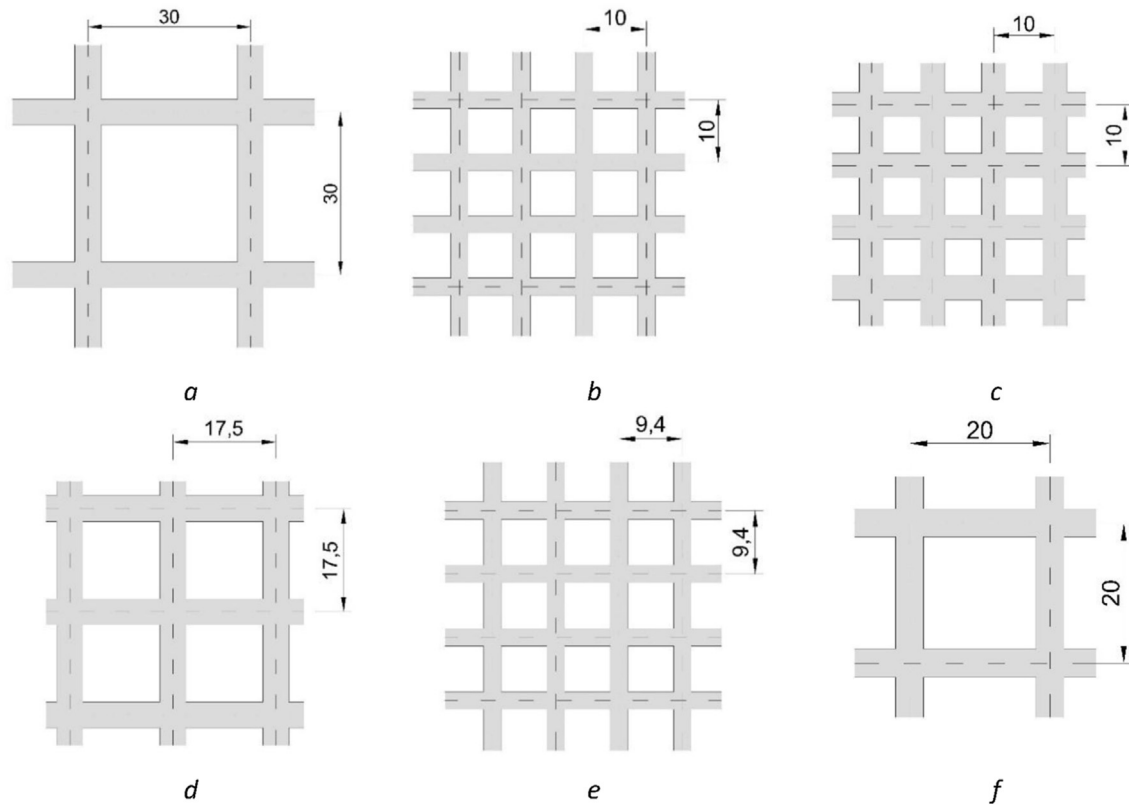


Fig. 1. Textile geometries: a) C_1; C_3; b) C_2; c) C_4; d) C_5a; e) C_5a; C_5b; f) C_6 [dimensions are expressed in mm].

Table 1
Mechanical properties of the components.

FRCM system	University or Research Institution	Textile		Matrix*		
		Tensile strength [MPa]	Modulus of elasticity [GPa]	Compressive strength [MPa]	Tensile strength** [MPa]	Modulus of elasticity [GPa]
C-FRCM_1	Certimac (Certimac) University of Patras (UPatras)	1800 ^c	227 ^c	10.3 ^c –12.0 ^{d.s.}	5 ^c	10 ^{d.s.}
C-FRCM_2	Cracow University of Technology (CUT) University of Bologna (UniBO)	3400 ^{d.s.}	240 ^{d.s.}	6.5 ^{d.s.} –9.8 ^d	3.8 ^d	N.A.
C-FRCM_3	Cracow University of Technology (CUT) University of Lyon (UniLyon)	1800 ^c	227 ^c	14.2 ^e –16.7 ^f	5.5 ^e	N.A.
C-FRCM_4	Politecnico di Milano (PoliMi) Roma3 University (UniRM3) University e Campus (UnieCampus)	1944 ^a –1890 ^b	203 ^a - 197 ^b	20 ^{d.s.}	N.A.	7 ^{d.s.}
C-FRCM_5a/b	University of Padova (UniPD): 5a University of Salento (UniLE): 5b	2500 ^{d.s.}	230 ^{d.s.}	38 ^{d.s.}	7 ^{d.s.}	16 ^{d.s.}
C-FRCM_6	University of Patras (UPatras) Roma3 University (UniRM3)	1876 ^b –1890 ^c	187 ^b - 219 ^c	16.4 ^c	6.7 ^c	15 ^{d.s.}

* The tests were performed at an age of 28 days.

** These results are obtained by flexural tensile tests.

^a Test performed by PoliMi.

^b Test performed by UniRM3.

^c Test performed by UPatras.

^d Test performed by UniBo.

^e Test performed by CUT.

^f Tests performed by UniLyon.

^{d.s.} Data reported in the data sheet.

Results C-FRCM_5 was considered for carbon FRCM used by Bernat-Maso et al. 2014 because the textile is uncoated and the matrix compressive strength is similar (38 MPa vs. 34.5 MPa)

3. Tensile tests

3.1. Preparation of specimens

The specimens were rectangular in shape and were either cast in single moulds or they were cut from a panel. No particular

treatments were applied during the preparation and curing phase. Only the specimens produced at Roma3 University and at Certimac were kept moist for 48 h in the moulds, then they were demoulded and immersed in water for 26 days. After extraction from water, the specimens were left in laboratory conditions for at least 7 days prior to testing.

In Table 2, the curing conditions and the age at testing are reported. These data could be very important in the analysis of the mechanical properties of the matrix and of the bond characteristics between matrix and textile. The age at testing varies between 35 and 153 days, the conditions are similar between the laboratories, but it is important to highlight that the specimens used at Roma3 University and at Certimac were immersed in water for 26 days.

The specimens have a thickness of 6–14 mm, but the width and the length depend on the characteristics of the testing machine used and on the geometry of each textile. In Table 2, the geometry of the specimens and the number of longitudinal yarns per specimen are reported. The tensile coupons tested at the University of Salento have a different geometry because only the central part of the textile was impregnated with the matrix whereas at the extremities the textile is impregnated with epoxy resin and it is clamped by the testing machine.

3.2. Test set-ups and instrumentation

Various set-ups for tensile tests on FRCM specimens were developed [13,16,17,20]. The specimen production, dimension and shapes and load application may largely influence the stress–strain behaviour of these materials. In the following the different test set-ups involved are described.

It was important to pay attention to the alignment of the specimen to avoid that parasitic bending moments arise during load application.

Different gripping systems were used: the specimens tested at Certimac, CUT and UniPD were reinforced at the extremities with FRP wraps and clamped with two bolted steel plates (Fig. 2a). Special padding (abrasive mesh and rubber sheet) was used to prevent slippage between the polymer and the steel plates. The specimens tested in the other universities were reinforced at the extremities with FRP materials for a length equal to 70–110 mm. The extremities were inserted in the steel wedges of the testing machine and an appropriate pressure was applied in order not to damage the sample and guarantee the absence of slipping phenomena (Fig. 2b and c). Only in one case (UNISALENTO) the textile

at the extremities of the specimens was not furnished with matrix but was glued between FRP tabs and clamped by the wedges of the testing machine.

Table 3 reports the clamping systems and the instrumentation used. It should be highlighted that the test set ups chosen by CUT and UNIPD provided a free rotation capacity at the gripping areas.

Different techniques were used to measure the displacement and the deformation of the specimens. The external instruments involved are extensometers with a gauge length between 50 and 200 mm, linear variable displacement transducers (LVDTs), potentiometers, and digital image correlation (DIC) measurement techniques.

3.3. Experimental results and failure modes

The possible failure modes of FRCM materials undergoing uni-directional tension are shown in Fig. 3. “Type A” accounts for failure at the clamps; “Type B” corresponds to matrix cracking along the length of the specimen with eventual fibers rupture; “Type C” denotes the matrix cracking along the length of the specimen coupled with fibers slippage at the clamps.

Different failure modes were evidenced, due to the mechanical properties of the composite materials, the matrix-to-textile bond characteristics and the differences in the test set-up. Fig. 4 shows the failure modes observed for the different FRCM materials.

In the following section the results of tensile tests are discussed for each system and then compared. The outcomes from the different laboratories are compared, in particular the failure modes, the stress-strain behaviour, the values of stiffness and maximum stress of the different phases are analyzed. The influence of the specimens geometry and the experimental set-ups detailing on the failure modes are also discussed.

Table 4 shows the experimental results. The table reports the average values and the coefficient of variation of the slopes (E_1, E_2, E_3) of the three phases that characterize the stress-strain curves, the stresses ($\sigma_{T1}, \sigma_{T2}, \sigma_u$) and strains ($\epsilon_{T1}, \epsilon_{T2}, \epsilon_u$) reached at the end of each phase and the failure modes of each FRCM system tested.

Table 2
Geometry of the samples.

FRCM system	University	# tests	Length [mm]	Thickness [mm]	Width [mm]	Number of yarns	Textile cross section [mm ²]	Curing/storing conditions and age at testing
C-FRCM_1	CERTIMAC	5	545	10	90	3	5.67	^b
		4	500	10	90	3	5.67	20° - 65% RH 62 days
C-FRCM_2	CUT	6	500	6	54	6	2.82	–
		5	500	6	54	6	2.82	20 °C 150 days
C-FRCM_3	CUT	5	595	10	96	3	5.67	21 ± 2 °C - 60 ± 10% RH 44 days
		5	650	10	108	3	5.67	20–25 °C - 50–60% RH 35–45 days
C-FRCM_4	POLIMI	5	400	9	40	4	1.88	20 °C–50–60% RH 35–45 days
		5	600	10	50	5	2.35	^b
		5	600	10	115	12	5.64	20–25 °C 204 days
C-FRCM_5 a	UNIPD	8	399	14	40	4	2.30	21 °C–68% RH <2 months
C-FRCM_5 b	UNISALENTO	4	260 ^a	12	100	5	3.60	20 °C–50% RH 58 days
C-FRCM_6	UNIRM3	5	600	10	50	2	2.35	^b
		5	500	10	60	3	2.82	20° - 65% RH 47 days

^a The geometry of the samples tested by UniSalento was different from the others.

^b Specimens were kept moist for 48 h in the moulds, then demoulded and immersed in water for 26 days. After extraction from water, specimens were left in laboratory conditions (about 20–25 °C and 50–60%RH) for 7 days (UniRM3) or 125 days (Certimac) prior to testing.

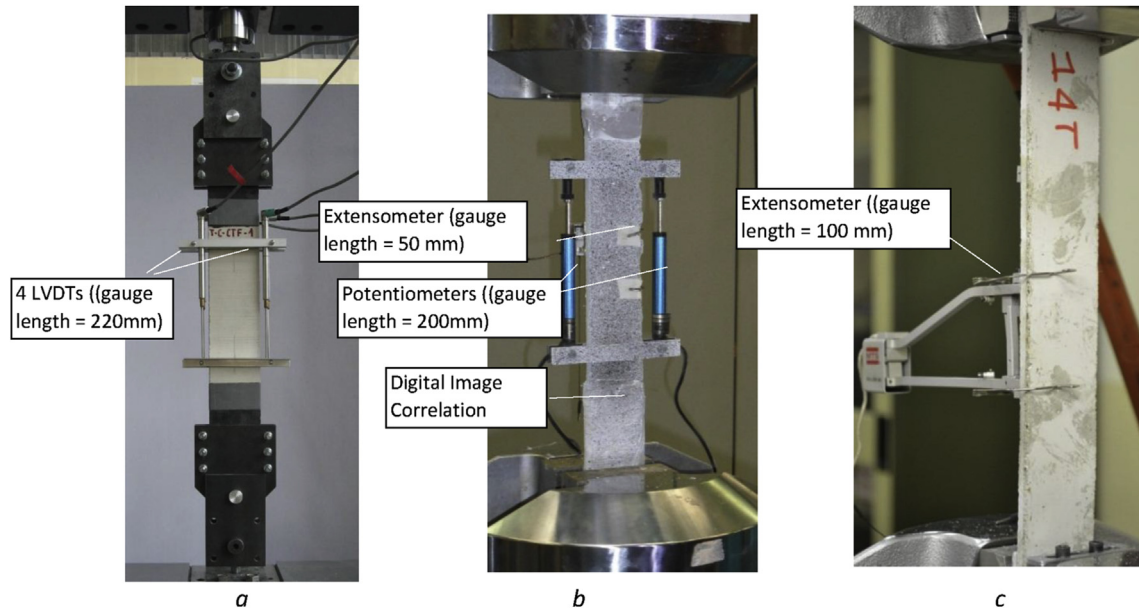


Fig. 2. Experimental set-up: a) CUT; b) UniRM3; c) PoliMi.

3.3.1. C-FRCM_1

The results of the tests performed at the University of Patras and at the laboratory of Certimac are different, in particular in the last phase (Fig. 5a). The tests performed at the University of Patras present a trilinear behaviour in which the second phase is quite pronounced and characterized also by spalling of the mortar. The third phase is characterized by a slope similar to the elastic modulus of the bare textile and a maximum stress equal to 58% of the tensile strength of the latter. The fact that the specimens ends were wrapped with FRPs increased locally the strength of the mortar and delayed its crushing in the gripping area preventing the slippage of the textile. The results of the tests performed at Certimac are characterized by a trilinear behaviour, in which the last phase is characterized by slippage between fibers and matrix located at the clamping wedges. For this reason, the maximum stress obtained is very low. This failure mode could be caused by the clamping method that involves the use of knurled plates bolted together with a tightening torque equal to 12 kNm without reinforcement of the specimens at the extremities. In Fig. 5a, the stress-strain curves are compared.

3.3.2. C-FRCM_2

The tests were performed at UniBo and CUT. Despite the fact that the clamping methods were different, the experimental results are in good agreement. The stress-strain curves could be considered tri-linear, even if the second and third phases present a similar slope. In Fig. 5b the stress-strain curves are compared. The maximum stress reached is equal to approximately 75% of the tensile strength of the bare fibers (the tensile strength reported by technical data sheet was used for the comparison).

Both for the tests performed by UniBo and CUT the failure mode was the cracking in the length of the specimen and fibers tensile failure.

3.3.3. C-FRCM_3

The results of the tests performed at the Universities of Lyon and Cracow present some differences, in particular in the last phase (Fig. 5c). The tests performed at the University of Lyon present a bi-linear behaviour in which the second phase is characterized by slippage phenomena between textile and matrix. The maximum

stress is equal to approximately 26% of the fibers tensile strength.

The results of the tests performed at CUT present a trilinear behaviour in which the last phase is characterized by slippage between the fibers and the matrix located at the clamping wedges. This phenomenon is not visible in the stress-strain plot because it occurred out of the LVDTs gauge length. Due to the failure mode, the slope of the first phase and the maximum stress are very low and equal to approximately 22% of the tensile strength and 25% of the elastic modulus of the dry fibers obtained by tensile tests on single yarn.

3.3.4. C-FRCM_4

Experimental tests on C-FRCM_4 were performed at UniRM3, PoliMi and UnieCampus. The results obtained by the three universities are comparable; the stress-strain behaviour is trilinear (Fig. 5d). The typical failure mode is characterized by a homogeneous crack distribution along the length of the specimens and by fibers rupture. Slippage phenomena between fiber filaments (telescopic slippage) and between fibers and matrix were noted in the last phase of the test. Damage of carbon textile was observed close to the main cracks or at the clamps. It was observed that failure did not occur at one section for all filaments in the yarns. Single filaments ruptured at different sections, which sometimes differed from the sections where the main cracks appeared. In particular in the tests performed at UniRM3 University it was possible to note that the single wires broke in different sections, generally different even from the section where the mortar matrix cracked. The tests performed at UniRM3 resulted in a higher stress at the end of the first phase. If these values are computed considering the nominal cross-section of the matrix, the average values of the maximum stress reached is 6.26 MPa for UniRM3, 2.37 MPa for PoliMi and 3.02 MPa for UnieCampus.

The slope of the third phase is very similar to the one of the bare textile for the tests performed at PoliMi, whereas it is lower for the tests performed at Roma3 University and UnieCampus (115 GPa and 154 GPa, respectively), maybe due to slippage phenomena occurred between textile and matrix.

It could be interesting also to note that the ultimate stress reached is equal to approximately 85% and 77% of the tensile strength of the dry fibers textile for the tests performed at PoliMi

Table 3
Clamping methods and instrumentation.

Material	University	Clamping method	Instrumentation	Test rate [mm/min]
C-FRCM_1	CERTIMAC	Knurled plates (width 120 mm; height 115 mm)	Extensometer (gauge length = 200 mm)	0.30 (un-cracked phase) 0.50 (cracked phase)
	UPATRAS	CFRP wraps and hydraulic clamping system of the testing machine	LVDTs (gauge length = 200 mm)	0.24
C-FRCM_2	CUT	The ends of the specimens were embedded in polymer layer (150 mm) and clamped with two bolted steel plates	LVDT (gauge length = 200 mm)	0.30
	UNIBO	FRP tabs and hydraulic clamping system of the testing machine	Extensometer (gauge length = 200 mm) DIC	0.20
C-FRCM_3	CUT	The ends of the specimens were embedded in polymer layer (150 mm) and clamped with two bolted steel plates	LVDT (gauge length = 200 mm)	0.30
	UNILYON	Aluminium tabs glued to the specimen ends and inserted inside hydraulic grips	LVDT (gauge length = 200 mm)	0.30
C-FRCM_4	POLIMI	FRP tabs (length = 60 mm) and hydraulic clamping system of the testing machine	Extensometer (gauge length = 100 mm)	0.10 (un-cracked phase) 0.20 (cracked phase)
	UNIRM3	GFRP wraps (length = 110 mm) and hydraulic clamping system of the testing machine	Extensometer (gauge length = 50 mm) Potentiometer (gauge length = 200 mm) DIC	0.60
	UNieCAMPUS	GFRP tabs and hydraulic clamping system of the testing machine	LVDT of the testing machine Digital Image Correlation	1.00
C-FRCM_5 a	UNIPD	Clevis Type: Two couples of steel plates glued to the ends with quick-setting resin, then bolted	Potentiometer (gauge length = 200 mm)	0.30 (un-cracked phase) 0.30–0.60 (cracked phase)
C-FRCM_5 b	UNISALENTO	Tabs applied on dry textile and hydraulic clamping system of the testing machine	LVDT of the testing machine	0.30
C-FRCM_6	UNIRM3	GFRP wraps (length = 110 mm) and hydraulic clamping system of the testing machine	Extensometer (gauge length = 50 mm) Potentiometer (gauge length = 200 mm) DIC	0.60
	UPATRAS	CFRP wraps and hydraulic clamping system of the testing machine	LVDTs (gauge length = 200 mm)	0.24

and UnieCampus, respectively, whereas it is equal to approximately 135% for the tests performed at UniRM3.

These specimens show a similar global behaviour, but with large differences in values obtained, which are mainly attributed to the different curing conditions and clamping systems. In particular, the samples tested at Roma3 University were kept moist for 48 h in the moulds, then demoulded and immersed in water for 26 days. After extraction from water, specimens were left in laboratory conditions (approximately 22 °C and 60% RH) for at least 7 days. The other samples were cured in laboratory conditions for at least 28 days. In this case, some micro-cracks due to a differential shrinkage could appear; instead in the first one shrinkage phenomena were prevented, and a better impregnation between textile and matrix was achieved. Another cause could be the different pressure applied to the clamps. In particular, in the tests performed at Roma3 University a higher pressure was applied, and this could produce a more homogeneous stress distribution in the filaments of the yarns. It is possible to hypothesize that the curing conditions and the stresses distribution at the clamps allowed to transfer the stresses to all the filaments in the yarns, and to reach a maximum stress higher than the one obtain with tensile tests performed on the bare textile. In the tests on non-impregnated textile the failure mode was characterized by the rupture of some filaments, and so the maximum stress could be underestimated.

3.3.5. C-FRCM_5

It is difficult to compare results of the tests performed on systems C-FRCM_5a and 5b because the textiles presented different mesh spacing, and the geometry of the specimens was completely different. In particular, in the specimens used at the University of Salento, FRP tabs were epoxy-bonded to the bare textile ends and clamped by the testing machine. In these tests the failure was characterized by cracking of the mortar and textile rupture. The elastic modulus of the first phase reported in Table 4 is not comparable with the elastic modulus of the mortar, due to the test set-up adopted.

The samples tested at the University of Padova failed under mode “C”, with cracking near the clamps and textile slippage. The maximum stress reached is lower than the textile strength.

3.3.6. C-FRCM_6

The tests on C-FRCM_6 were performed at the universities of Patras and Roma3. The results are comparable, the stress-strain curves exhibit a tri-linear behaviour in which the second phase is not well recognizable because the appearance of cracks caused stress drops also in the third phase (Fig. 5f). The failure modes are different because in the tests performed at the University of Patras a homogeneous cracking along the specimen was initially noted, but the failure occurred due to the opening of a major crack near the clamps, which was followed by fibers slippage. These results are presented and deeper described in Ref. [35]. For some tests performed at Roma3 University failure occurred in the mid-span of the specimen, while in others close to the gripping areas. Generally, the crack pattern at failure was characterized by three cracks at about 90 mm distance from each other. It was observed that failure did not occur in one section for all the filaments comprised in the yarns; the single filament brakes in different sections that could be also different from the section where the main cracks appeared. It is possible to note that the stress reached at the end of the first phase is slightly higher than the matrix tensile strength. Besides, maximum stress values obtained were higher than the textile strength (approximately 140% of the textile strength). From the analysis of the tests performed on the bare textile, it is noted that in many cases failure involves only some filaments in the yarns. Maybe for this reason the textile strength is lower than the maximum stress obtained with tests on FRCM specimens, where failure of all yarn filaments was observed.

3.4. Comment and comparison

In this section an analysis of the main parameters that influence the experimental results and a comparison among the efficiency of

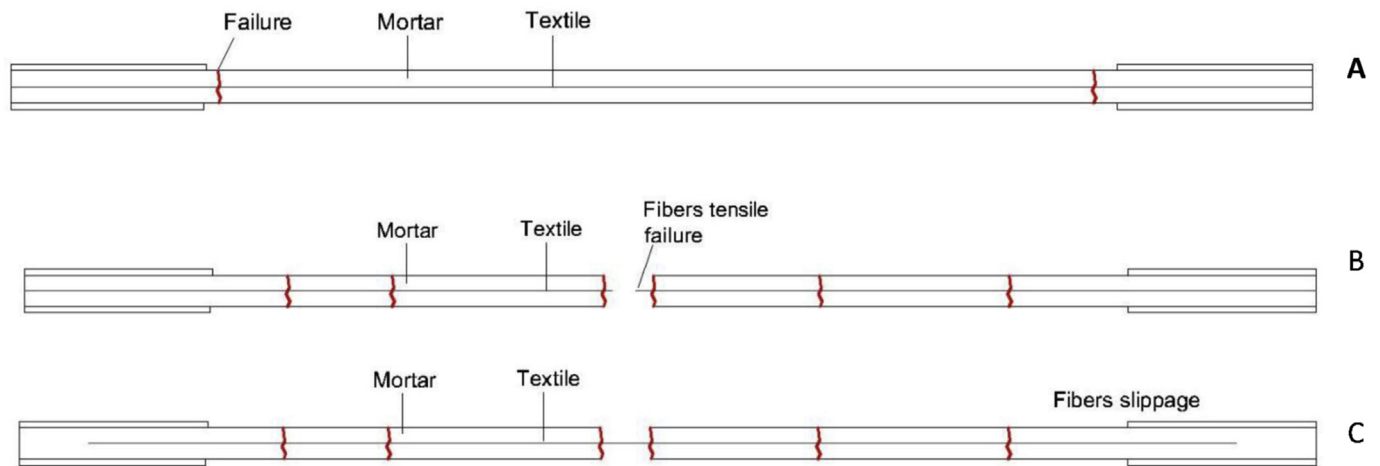


Fig. 3. Possible failure modes (unidirectional tensile loading).

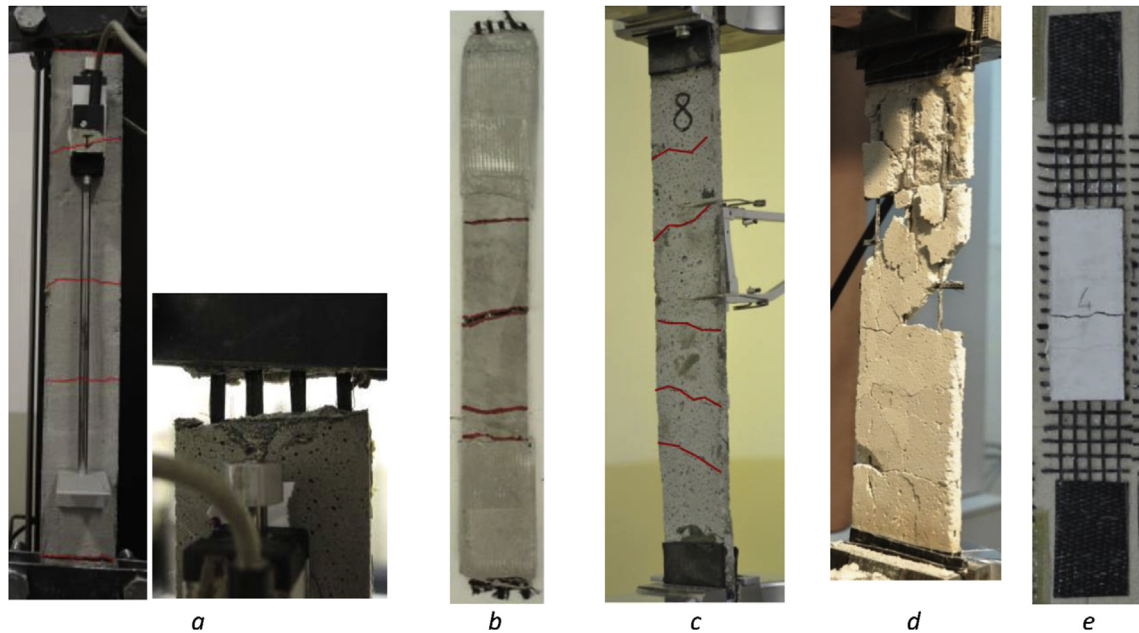


Fig. 4. Example of failure modes: a) C-FRCM_5a tested by UniPD; b) C-FRCM_4 tested by UNIRM3 c) C-FRCM_4 tested by PoliMi; d) C-FRCM_1 tested by UPatras; e) C-FRCM5 tested by UniSalento.

the different systems analyzed are reported.

3.4.1. Test instrumentation and clamping method

Three main clamping methods were involved in the experimental campaign:

- The extremities of the specimen were strengthened with FRP wraps or tabs and clamped by the wedges of the testing machine.
- The ends of the specimen were strengthened with polymer and clamped with two bolted steel plates. In some cases, to prevent slippage between the polymer and the plates and to avoid damages in the mortar, some additional layers were used (abrasive meshes and rubber sheet).
- At the extremities of the specimen the textile remained bare, FRP tabs were applied on the textile and clamped by the wedges of the testing machine.

Clevis type grips were used only by UniPD, even if the tabs used are bolted together and not glued at the end of the specimen. The use of this clamping method is recommended by the American acceptance criteria [6] and is preferred to reproduce the actual behavior that FRCM materials present in the field, but it doesn't permit to have a full characterization of the FRCM system and the develop of its full tensile load-bearing potential [20]. As expected, the tests performed with clamping method "c" present a stress-strain curve completely different when compared to the other ones. In the first phase of the test the textile is the only carrier of the tensile load; when the stress is transferred to the mortar only one crack appears in the central part of the specimen. Clamping methods "a" and "b" could be considered comparable, but attention should be paid in the choice of the pressure applied at the extremities of the sample, in order to prevent both slippage phenomena between textile and matrix and cracking of the mortar near the clamps. Also, the choice of the material used to reinforce

Table 4

Tensile tests: experimental results.

System	Laboratory		E_1 [GPa]	E_2 [GPa]	E_3 [GPa]	σ_{T1} [MPa]	σ_{T2} [MPa]	σ_u [MPa]	ϵ_{T1} [%]	ϵ_{T2} [%]	ϵ_u [%]	Failure mode ^a
C-FRCM_1	UPATRAS	Average	131.3	17.0	245.0	92.0	282.8	1043.3	0.10	1.30	1.98	C
		CoV [%]	124.6	25.0	42.2	27.3	27.2	2.0	135.3	29.6	13.0	
	CERTIMAC	Average	–	–	–	86.1	–	227.2	0.48	–	1.18	A + C
		CoV [%]	–	–	–	50.5	–	11.6	50.2	–	40.6	
C-FRCM_2	CUT	Average	440.2	217.1	190.0	149.0	521.3	2617.1	0.03	0.21	1.33	B
		CoV [%]	7.3	3.6	4.0	3.5	3.4	9.0	5.0	–	7.5	
	UNIBO	Average	387.1	186.2	222.0	192.1	1287.0	2396.1	0.05	0.64	1.14	B
		CoV [%]	18.6	1.9	3.0	9.8	5.5	5.0	17.0	7.1	4.4	
C-FRCM_3	CUT	Average	2941.3	–	94.3	265.3	–	404.3	0.01	–	0.53	C
		CoV [%]	39.5	–	47.4	41.7	–	13.4	15.2	–	36.8	
	UNILYON	Average	657.5	106.7	–	364.3	459.9	–	0.06	0.22	–	A (+C)
		CoV [%]	29.0	18.0	–	9.0	12.0	–	30.0	60.0	–	
C-FRCM_4	POLIMI	Average	989.5	73.1	209.6	504.4	653.4	1635.1	0.05	0.23	0.76	B
		CoV [%]	23.5	28.6	20.3	22.9	23.2	14.0	10.2	22.4	17.7	
	UNIRM3	Average	1782.2	65.7	154.6	1331.8	1471.6	2587.5	0.10	0.33	1.11	B + A
		CoV [%]	54.8	70.7	4.5	3.4	20.7	5.9	23.2	20.4	6.4	
	UNIECAMPUS	Average	1387.1	22.1	114.7	617.3	643.8	1484.5	0.05	0.20	1.15	C
		CoV [%]	18.2	5.2	38.4	20.7	22.6	7.0	9.0	57.8	16.7	
C-FRCM_5	UNIPD	Average	2168.3	–	206.5	567.3	671.7	979.6	0.03	0.52	0.72	C
		CoV [%]	17.0	–	10.1	5.7	17.2	4.3	11.4	7.8	18.2	
	UNISALENTO	Average	(73.0) ^b	115.6	174.8	287.4	271.2	1592.2	0.46 ^b	0.39	1.46	B
		CoV [%]	27.1	11.1	28.1	16	24.2	21.2	33.1	37.1	14.0	
C-FRCM_6	UNIRM3	Average	5946.5	–	199.4	1551.8	–	2525.6	0.03	–	0.87	A + B
		CoV [%]	10.2	–	6.5	44.7	–	11.1	49.7	–	7.1	
	UPATRAS	Average	3426.0	70.0	196.2	1724.0	2376.3	2832.0	0.05	0.58	0.81	C
		CoV [%]	6.3	25.9	15.7	32.6	6.5	4.8	38.4	6.9	20.9	

^a The failure modes are described in Fig. 3.^b This value is not comparable with the other ones due to the different test set-up employed.

and pad the extremities is important in order to avoid compressive failure of the mortar.

To measure the strain during the tests, potentiometers, LVDTs and extensometers were used. In the tests performed using different type of measurement (e.g. tests performed at UniRM3) no evident scatters due to the different instrumentation were highlighted. It is important to note that, to correctly compute the uncracked stage, the first cracks developed on the specimen must be located within the gauge length of the instrument, and that the gauge length should be long enough to guarantee that a significant number of cracks (if not all) is recorded. In some cases also Digital Image Correlation technique (DIC) was used and the results were similar to the ones obtained with the external instruments.

3.4.2. Specimens geometry

The specimens geometry chosen in this project is prismatic with constant thickness (6–14 mm); the width is related to the free space between the yarns and to the number of yarns inserted, that should be chosen in order to limit non-uniform stress distribution in the textile. The length of the specimen was varied between 400 mm and 600 mm (if the samples used at UNISALENTO are not considered). Specimen length should not affect the results provided that it is enough to guarantee a uniform stress distribution among the yarns and avoid stress concentration at the clamps. Long lengths (higher than 600 mm) should be avoided to prevent problems in the curing phase, non-planarity of samples due to differential shrinkage of the two main surfaces and appearance of micro cracks in the matrix. It is more important to consider the ratio between the length of the sample and the gauge length of the instrumentation used to measure the strain. In fact, if the first cracks appear in the external part of the extensometer (or LVDT) the tests results should not be considered reliable. It seems that the number of yarns included in the specimens does not influence the results of the test if a homogeneous stress distribution is guaranteed between yarns.

3.4.3. Comparison between different FRCM systems

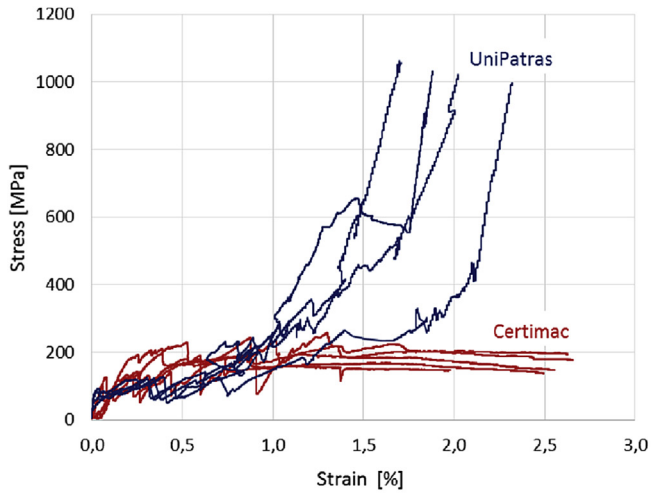
It could be noted that the test set-up has large importance in the experimental results and variability. In particular, it could be highlighted that the materials tested with hydraulic clamping and using FRP wraps (C-FRCM_2, C-FRCM_4 and C-FRCM_6) present the more satisfactory results. It should be considered that the curing conditions and the geometry may cause differences in the results. If we compare the results of different C-FRCM materials without considering the test set-ups, it is possible to note that the stress-strain behaviour is largely influenced by the mechanical properties of the textile and the matrix and by the geometry of the textile. Only in 2 or 3 cases the stress-strain behaviour can be represented by a tri-linear curve. In all cases, except for C-FRCM_2, after an initial uncracked phase, the behaviour is markedly non-linear.

In Fig. 6 a comparison between the experimental results performed on each system is reported. In particular, the stress and the corresponding strain reached at the end of each phase for the different systems was analyzed. The values reached at the end of each phase are represented with different symbols and may be compared with the textile strength represented by the horizontal dashed line.

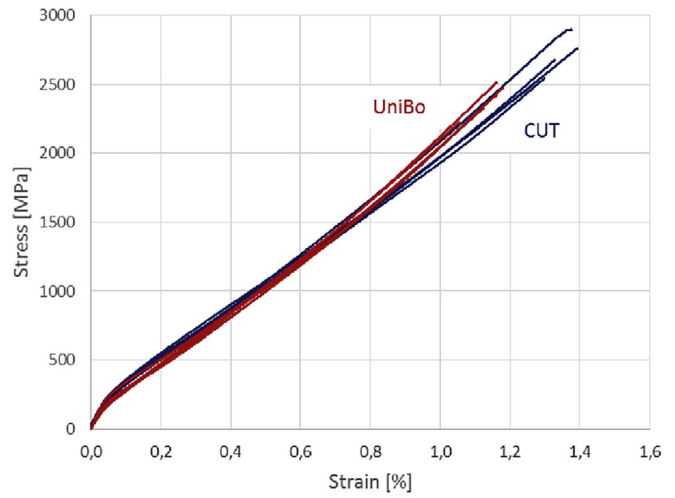
These plots permit to evaluate the scatter in the experimental results, to compare the stress reached at the end of each phase with the textile tensile strength and to compare the mechanical properties of the different systems.

It could be highlighted that for some systems it is not possible to identify the parameters related to each phase and that the scatter between the results can be very high. The variability of the results may be caused by many factors:

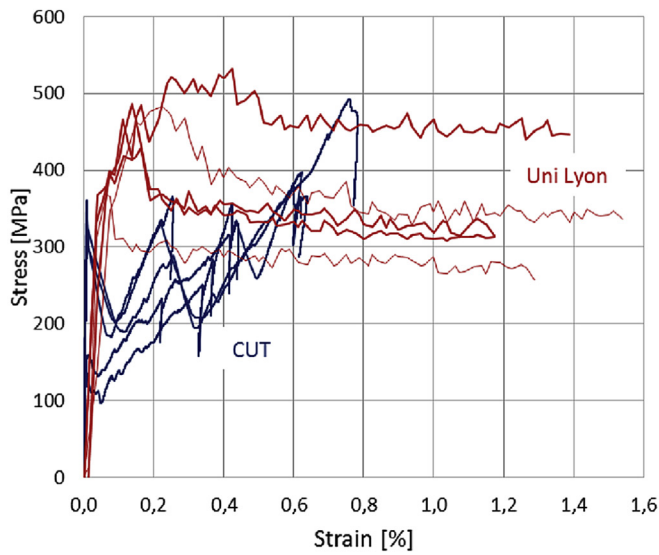
- Specimens properties: irregularity of the cross-section; presence of micro-cracks; misalignment of the textile with respect to the specimen mid-thickness, different thickness of the specimens.
- Instrumentation: position of the first cracks. If micro-cracks appear outside the gauge length of the extensometer during



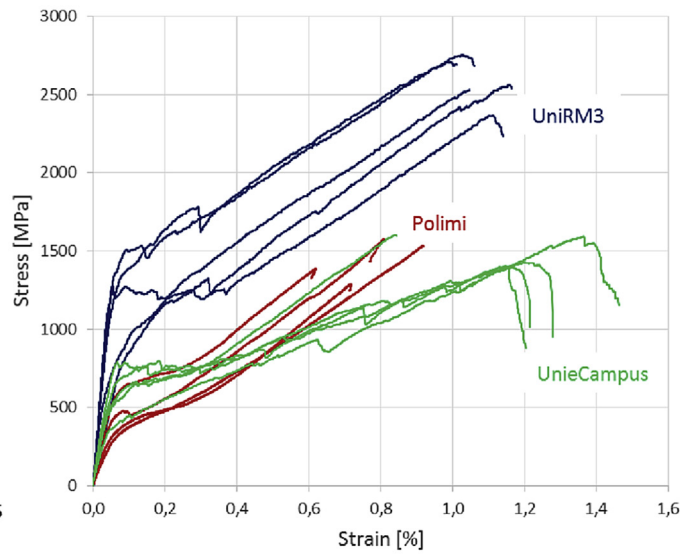
a



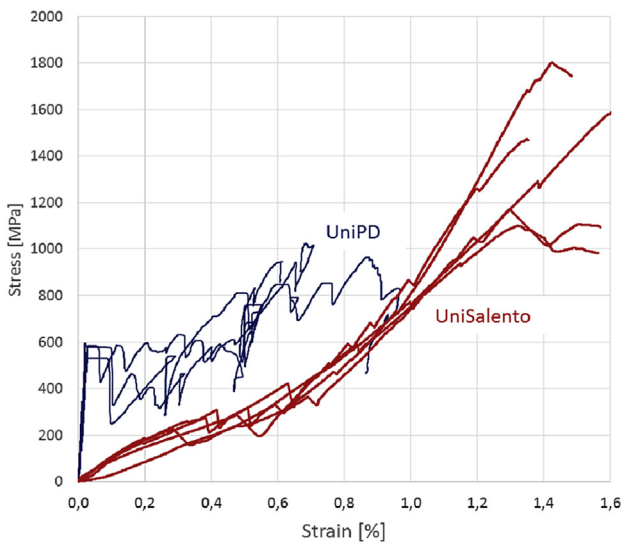
b



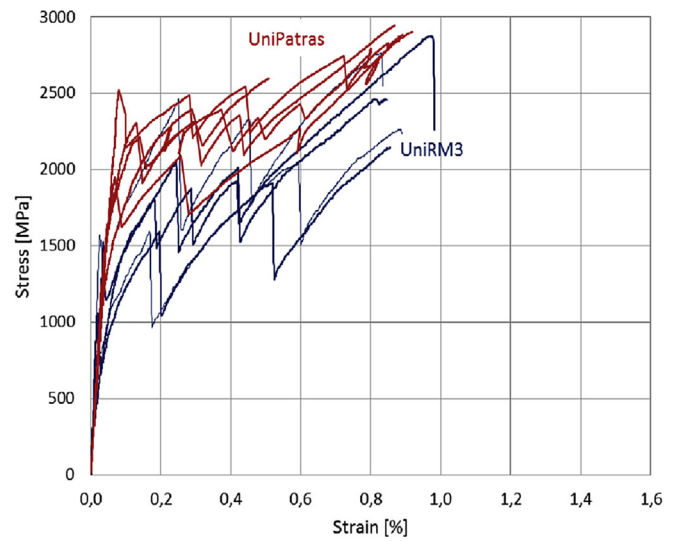
c



d



e



f

Fig. 5. Tensile tests: stress-strain behaviour: a) C-FRCM_1; b) C-FRCM_2; c) C-FRCM_3; d) C-FRCM_4; e) C-FRCM_5; f) C-FRCM_6.

the elastic phase, the elastic modulus of the first phase measured could vary a lot.

- Clamping method: the pressure at clamping should prevent slippage phenomena between textile and matrix at the clamps.
- Failure mode: the maximum stress and the stiffness could be influenced by slippage phenomena between textile and matrix.

4. Shear tests

4.1. Properties and preparation of specimens

For standardization purposes as well as to permit the comparison among different mortar-based reinforcement systems, the substrates used in this work (masonry) have the same mechanical properties and geometry.

The same type of solid clay bricks was used, characterized by the following mechanical properties: compressive strength: 14.8 MPa, elastic modulus: 5760 MPa, tensile strength: 2.5 MPa [22]. Mortar joints with a thickness of approximately 10 mm and a compressive strength not higher than 5 MPa were used. The masonry prisms are composed by five stack-bonded bricks or five half bricks and four mortar joints. The dimensions of the substrate wallettes and of the reinforcement strips are reported in Table 5.

In some cases, the masonry prisms were made by the manufacturer of the tested composite materials, in others by the university laboratories. No primer or other surface treatments were applied on the substrate. The substrate surface was cleaned from dust with compressed air and saturated with water before matrix application.

A single-lap configuration was chosen by all laboratories. The reinforcement was located at a distance between 10 and 30 mm from the upper face of the bricks and at least 20 mm from the sides. The bond length was equal to 260 mm and the bond width ranged between 40 and 100 mm. The bond length was chosen based on the available literature [21,23] in the attempt to develop the entire joint load corresponding capacity. On the other hand, larger dimensions were not selected to avoid space issues with the testing equipment.

The thickness of the reinforcement system was similar to the one of the specimens used for the tensile tests, and representative of the thickness used in real-life strengthening applications, equal to approximately 10 mm.

In some cases (UniSALENTO, UniBO), the textile outside the bond length was impregnated with epoxy resin in order to provide a uniform load distribution.

4.2. Test set-ups and instrumentation

The specimens (masonry prisms with an externally bonded FRCM strip on one side) were placed in a steel frame stiff enough to limit rotations and deformations. A careful positioning of the specimen was necessary to ensure the load alignment respect to the longitudinal axis of the textile strip. By doing so, the load was applied to the textile and the development of parasitic stresses normal to the substrate-to-matrix interface was prevented. This test set-up requires particular care in clamping the free end of the strip. Three main clamping methods were used. In the first one two aluminum or FRP tabs were glued to the bare textile end and clamped by the wedges of testing machine. The second and third methods involved the use of two metal plates between which the textile was bolted; the end part of the textile was reinforced with polymers or FRP tabs. The clamping system could be directly inserted into the wedges of the testing machine or connected to a cylindrical or spherical joint.

In order to measure the relative slippage between textile and substrate, a metal profile was glued to the textile at the loaded end

of the composite strip, and different instruments like LVDTs or potentiometers were used. All the tests were performed under displacement control, the test rate varied between 0.15 mm/min and 0.30 mm/min (except for the tests performed at UniPD) as showed in Table 6.

The different set-up characteristics, the geometry of the samples, the instrumentation and the test rate could influence the test results [33,36]. In this first phase a unique testing procedure was not imposed in order to analyze the influence of the different set-ups and of the equipment of a large number of laboratories.

Table 6 shows the different clamping methods and the instrumentation adopted, in Fig. 7, some examples of the different test set-ups are illustrated.

4.3. Experimental results and failure modes

The possible failure modes that could be obtained by a shear test on FRCM materials are presented in Fig. 8. "Type A": debonding of the reinforcement system with cohesive failure within the substrate; "Type B": detachment at the matrix-to-substrate interface; "Type C": debonding at the textile-to-matrix interface; "Type D": textile slippage within the matrix; "Type E": textile slippage and cracking of the outer layer of mortar; "Type F": tensile failure (rupture) of the textile. Different failure modes were observed, due to the mechanical properties of the composite materials tested, the textile-to-matrix bond properties and the test set-up detailing (see Fig. 9).

In the following sections the results of shear tests are discussed for each system and then compared. The outcomes from the different laboratories are compared on the basis of the derived stress-slip curves. The influence of the FRCM strips geometry and the experimental set-ups on the observed failure modes are also discussed.

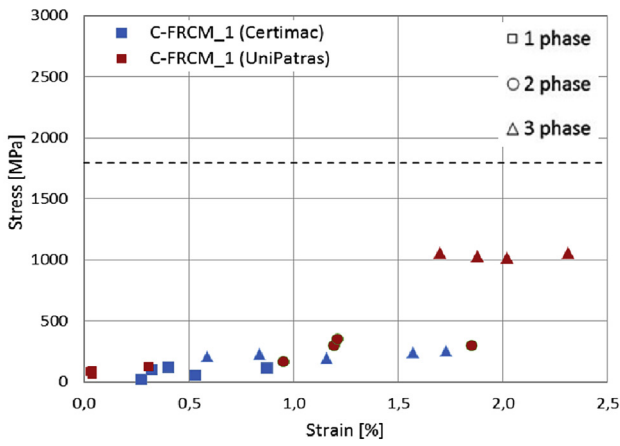
Table 7 shows the experimental results. All parameters are computed with reference to the cross-sectional area of the fibers. The exploitation ratio (σ_{\max}/f_T) was computed as the ratio between the maximum stress obtained by the shear tests (σ_{\max}) and the tensile strength obtained by tensile tests on the fibers (f_T).

4.3.1. C-FRCM_1

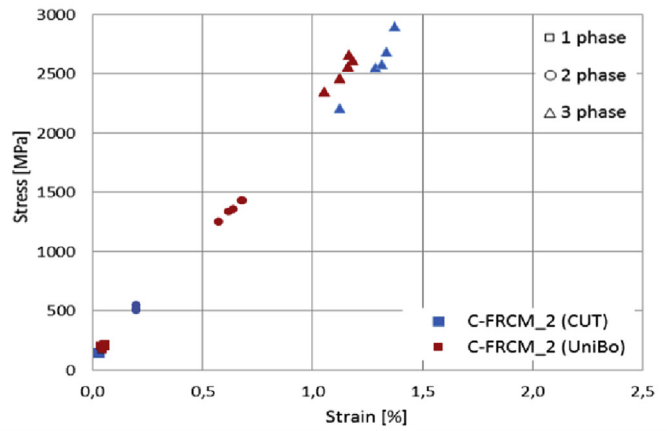
The tests performed at the University of Patras on C-FRCM_1 resulted in failure modes "B + E" and "E", with cracking of the mortar right above the transversal yarns that were stitch-bonded to the longitudinal ones. In some cases the detachment of a portion of the composite from the substrate was also observed. The tests performed at Certimac resulted in two cases of failure mode "E" with a crack in the final part of the FRCM strip, and in three cases of failure mode "F". The curves present a large scatter, with coefficients of variation between 30% and 48%. In Fig. 10a the stress-slip curves obtained by the two laboratories are reported; the stress drops visible in the first phase are due to the appearance of cracks in the mortar. The exploitation ratio is approximately 25% of the tensile strength of the corresponding textile.

4.3.2. C-FRCM_2

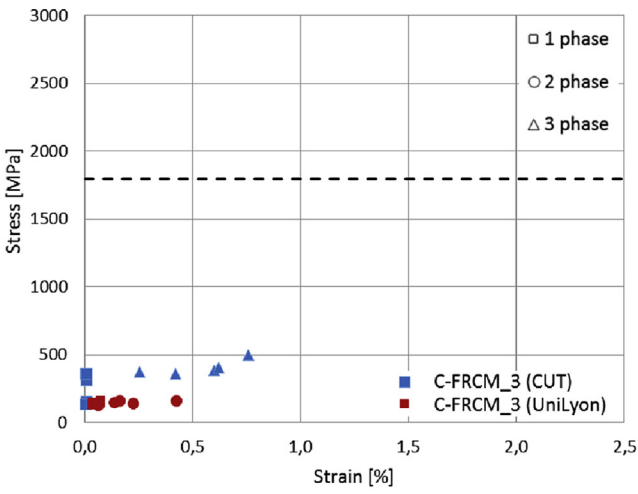
The tests performed at the Universities of Bologna and Cracow produced similar results (Fig. 10b). The typical failure mode evidenced by UniBo was debonding in the internal (i.e. in contact with the substrate) layer of mortar, whereas at CUT failure modes type "C", "A" (limited to a little portion at the free end) and "F" were observed. In particular, in many cases cracking of the mortar matrix was observed, in particular longitudinal cracks at the matrix-textile interface. In two cases textile failure was observed before cracking of the mortar. It should be noted that a local cohesive failure of the substrate at the loaded end (on the 5th brick) occurred in one test.



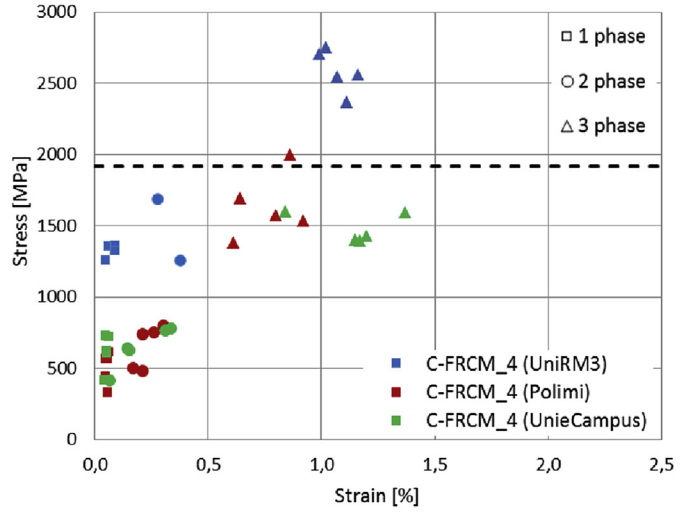
a



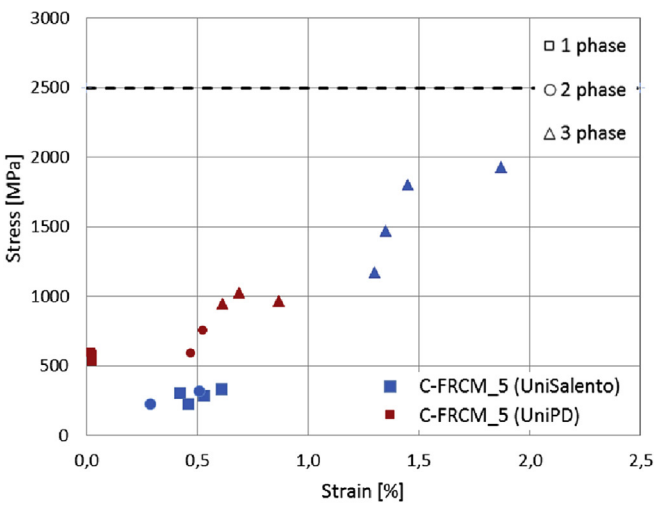
b



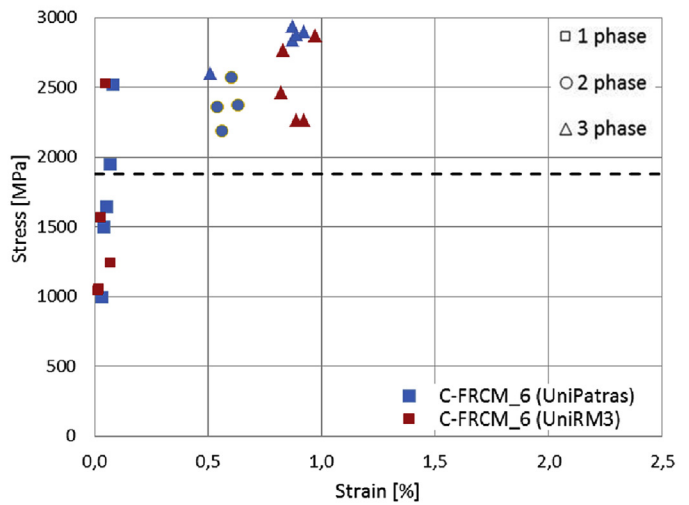
c



d



e



f

Fig. 6. Comparison between stress-strain results: a) C-FRCM_1; b) C-FRCM_2; c) C-FRCM_3; d) C-FRCM_4; e) C-FRCM_5; f) C-FRCM_6; the dashed line indicates the textile tensile strength.

Table 5
Specimens geometry.

Material	University	# tests	Substrate dimensions [mm]	FRCM bond length [mm]	FRCM bond width [mm]	Number of yarns (warp)	Number of yarns (weft)
C-FRCM_1	CERTIMAC	5	250 × 120 × 315	260	90	3	20
	UPATRAS	5	250 × 125 × 315	260	90	3	8
C-FRCM_2	CUT	6	250 × 120 × 315	260	54	6	28
	UNIBO	5	125 × 120 × 315	260	54	6	29
C-FRCM_3	CUT	5	250 × 120 × 315	260	96	3	8
	UNILYON	5	250 × 125 × 290	260	108	3	9
C-FRCM_4	POLIMI	5	250 × 120 × 315	260	100	10	26
	UNIECAMPUS	5	200 × 120 × 315	260	100	12	28
	UNIRM3	5	125 × 120 × 315	260	50	5	25
C-FRCM_5a	UNIPD	5	120 × 120 × 310	260	38	4	27
C-FRCM_5b	UNISALENTO	5	250 × 120 × 315	260	100	4 or 5	14
C-FRCM_6	UNIRM3	5	125 × 120 × 315	260	50	2	11
	UPATRAS	5	250 × 125 × 315	260	60	3	13

Table 6
Clamping methods and instrumentation.

Material	University	Clamping method	Instrumentation	Test rate [mm/min]
C-FRCM_1	CERTIMAC	Knurled plates without any spherical joint	2 LVDTs	0.30
	UPATRAS	Bolted steel plates connected to the hydraulic wedges	2 LVDTs	0.18
C-FRCM_2	CUT	Bolted steel plates connected with a spherical joint	2 LVDTs	0.30
	UNIBO	Glued and bolted steel plates with a hinge for allowing rotations around the vertical axis	2 LVDTs DIC	0.15
C-FRCM_3	CUT	Bolted steel plates connected with a spherical joint	2 LVDTs	0.30
	UNILYON	Aluminium tabs glued to the textile ends and inserted inside a grab system	2 LVDTs	0.30
C-FRCM_4	POLIMI	Bolted steel plates connected with a spherical joint	2 LVDTs	0.30
	UNIECAMPUS	FRP tabs inserted in the hydraulic wedges	2 LVDTs	1.00
	UNIRM3	Aluminium tabs glued to the textile ends and inserted in the hydraulic wedges	2 LVDTs Extensometer DIC	0.18
C-FRCM_5a	UNIPD	Glued and bolted steel plates without any spherical joint	4 Potentiometers	0.30–0.60
C-FRCM_5b	UNISALENTO	Aluminium tabs glued to the textile ends and inserted in the hydraulic wedges	2 LVDTs	0.30
C-FRCM_6	UNIRM3	Aluminium tabs glued to the textile ends and inserted in the hydraulic wedges	2 LVDTs Extensometer DIC	0.18
	UPATRAS	Bolted steel plates connected to the hydraulic wedges	2 LVDTs	0.18

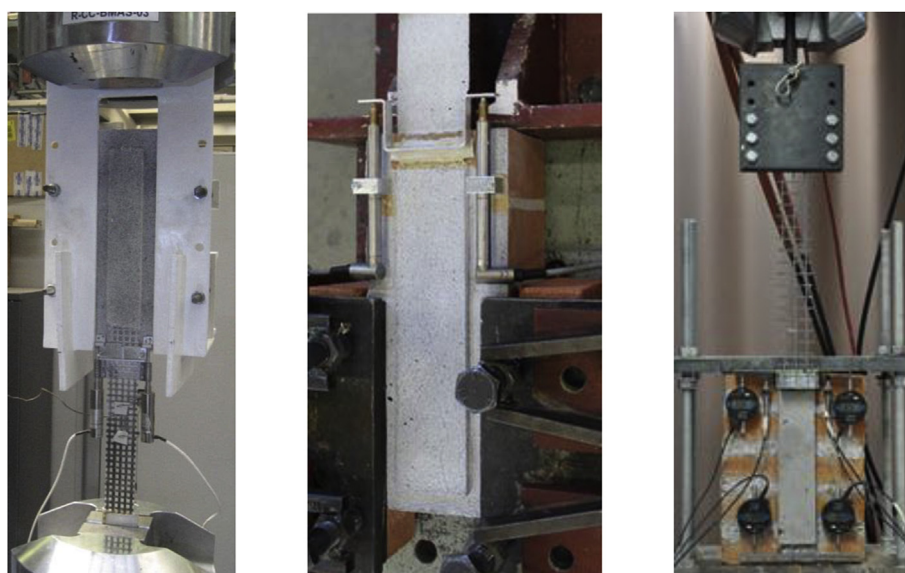


Fig. 7. Test set-ups: a) UniRM3; b) UniBO (the set-up was horizontal, the picture is rotated); c) UPatras.

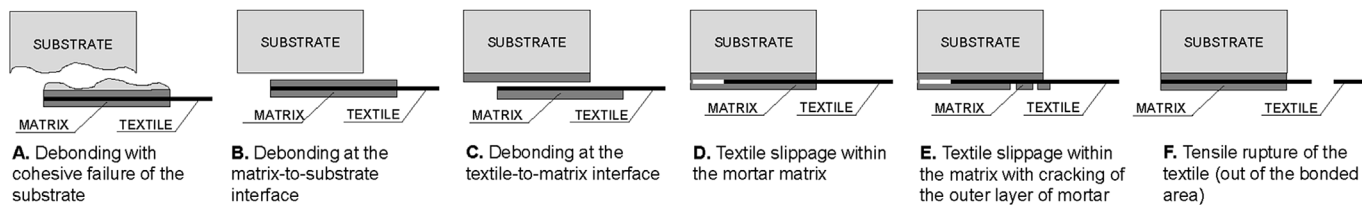


Fig. 8. Possible failure modes for externally bonded FRCM strips on solid substrates.

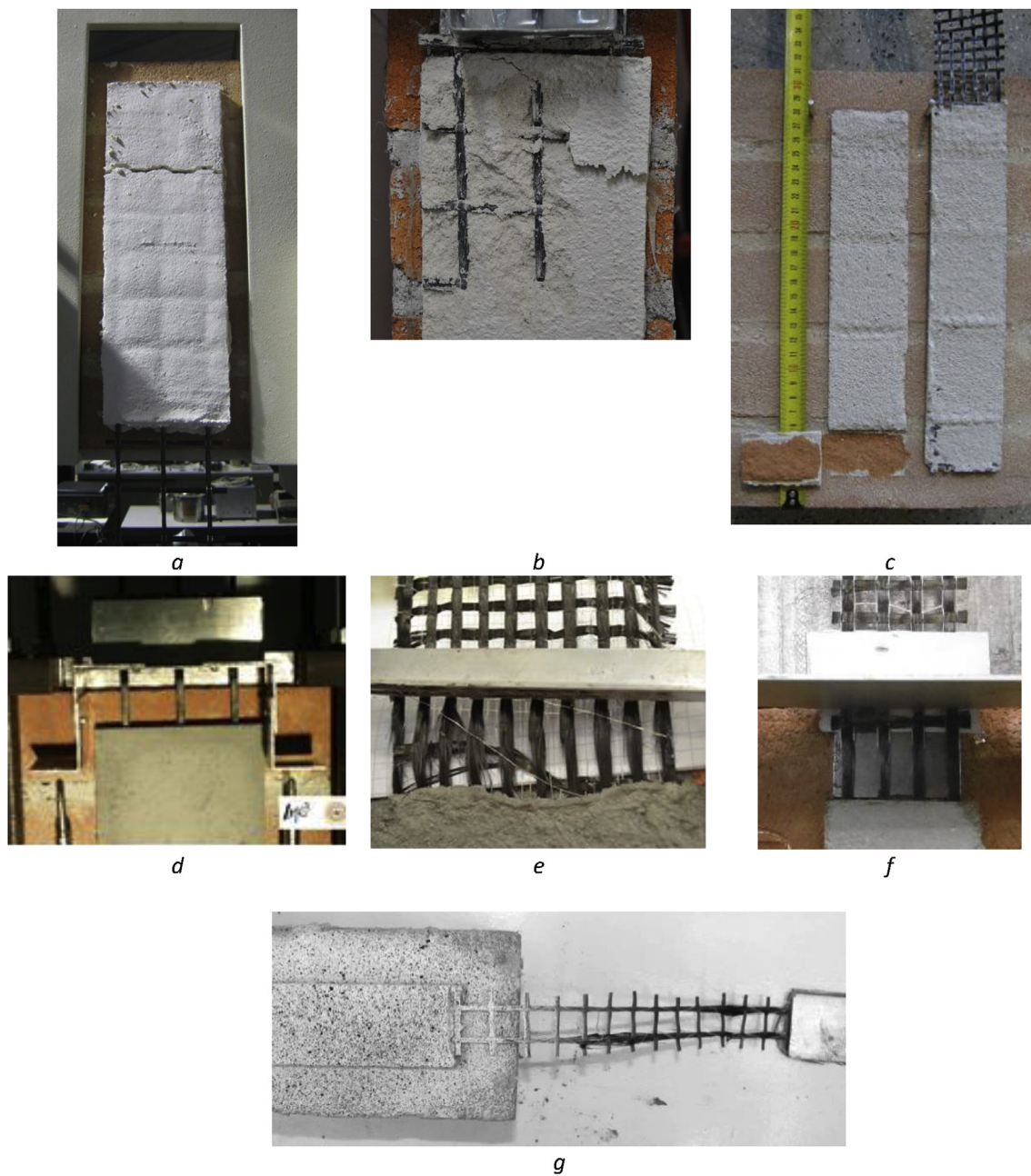


Fig. 9. Failure modes: a) C-FRCM_1 (Certimac) – Failure “E”; b) C-FRCM_1 (UPatras) – Failure “E”; c) C-FRCM_2 (CUT) – Failure “C”, “A”; d) C-FRCM_3 (UniLyon) – Failure “D”; e) C-FRCM_4 (PoliMi) – Failure “D”, “F”; f) C-FRCM_5 (UniPD) – Failure “F”; g) C-FRCM_6 (UniRM3) – Failure “F”.

Table 7
Shear tests: experimental results.

System	Laboratory	Bond width [mm]/n. yarns	Bond length [mm]/n. yarns		Peak load per unit width [N/mm]	Peak stress in the textile [MPa]	σ_{\max}/f_r	Slip at peak stress [mm]	Failure mode ^a
C-FRCM_1	UPATRAS	90/3 yarns	260/18 yarns	Average	34.3	544.6	30.3%	3.06	B + E
				CoV [%]	30.5			39.6	
C-FRCM_2	CERTIMAC	90/3 yarns	260/20 yarns	Average	26.3	416.8	23.2%	1.95	E/F
				CoV [%]	47.7			48.1	
C-FRCM_2	CUT	54/6 yarns	260/28 yarns	Average	65.8	1259.6	37.0%	0.72	C/A/F
				CoV [%]	14.1			71.4	
C-FRCM_2	UNIBO	54/6 yarns	260/29 yarns	Average	71.1	1361.2	40.1%	0.84	C
				CoV [%]	5.5			41.9	
C-FRCM_3	CUT	96/3 yarns	260/8 yarns	Average	41.4	701.4	38.9%	4.03	D/B
				CoV [%]	21.5			40.8	
C-FRCM_3	UNILYON	108/3 yarns	260/9 yarns	Average	15.0	286.2	15.9%	5.89	D
				CoV [%]	16.4			16.0	
C-FRCM_4	POLIMI	100/10 yarns	260/26 yarns	Average	42.7	1015.7	52.9%	0.91	D + F
				CoV [%]	11.4			41.5	
C-FRCM_4	UNIRM3	50/5 yarns	260/25 yarns	Average	63.9	1360.1	70.9%	1.08	F (+D)
				CoV [%]	6.9			15.1	
C-FRCM_4	UNIECAMPUS	100/12 yarns	260/28 yarns	Average	55.4	981.6	51.6%	0.6	D + F
				CoV [%]	9.6			56.6	
C-FRCM_5	UNIPD	38/4 yarns	260/27 yarns	Average	66.4	1079.8	43.2%	1.01	F
				CoV [%]	3.8			95	
C-FRCM_5	UNISALENTO	100/4–5 yarns	260/14 yarns	Average	26.2	753.6	30.1%	–	D
				CoV [%]	6.3			–	
C-FRCM_6	UNIRM3	50/2 yarns	260/11 yarns	Average	74.6	1587.6	85.2%	1.42	F
				CoV [%]	3.5			19.2	
C-FRCM_6	UPATRAS	60/3 yarns	260/13 yarns	Average	60.0	1330.2	70.3%	1.36	E
				CoV [%]	20.2			25.8	

^a Failure modes are described in Fig. 8.

The exploitation ratio is approximately equal to the 40% (referred to the tests performed on non-impregnated yarn).

4.3.3. C-FRCM_3

The tests performed at the University of Lyon failed under mode “D”, slippage of the textile within the matrix. It should be highlighted that in the tests performed at the University of Lyon a significant slippage occurred from early stage of the test, maybe due to problems in the manufacturing of the specimens. Only in one case a crack in the external layer of mortar was observed. The tests performed at CUT showed textile slippage in the matrix and, in two cases, debonding at the matrix-to-substrate interface and detachment of the FRCM strip. No cracks in the mortar were observed during the test. The maximum stresses reached in the tests are quite different, with an exploitation ratio equal to 39% for tests performed at CUT and equal to 16% for tests performed at Lyon. Also, the stiffness of the first phase is different: an average value of 378 N/mm was experienced at UniLyon, whilst a value of 9072 N/mm was obtained by the test performed at CUT. This difference in the experimental results was probably due to the manufacturing of the specimens or to the curing phase, a very weak bond between textile and the matrix was produced. In Fig. 10c both the experimental curves obtained by UniLyon and CUT are reported, even if they are not comparable.

4.3.4. C-FRCM_4

The failure mode reported by the laboratories that tested this material was slippage of the textile in the mortar layer and failure (rupture) of the textile near the loaded end of the bonded area. The stress-slip curves reported in Fig. 10d showed a similar behaviour, although an accurate measure of the specimens post-peak behaviour (descending branch of the curves) was problematic for PoliMi. It is noted that different textile widths were used between different labs. For large widths (100 mm) a rotation of the metal profile was observed (due to uneven load distribution) and the failure was mainly localized on one side of the textile. The exploitation ratio varies between 53% and 71%.

4.3.5. C-FRCM_5

The tests performed at the Universities of Padova and Salento resulted in two different failure modes. In the first case, failure occurred in the unbonded part of the textile at the beginning of the mortar; in the second one, failure occurred due to slippage of the textile within the matrix.

The test set-up used at University of Salento involved the measurement of the slip between the mortar and the substrate and so these tests are not comparable with those performed by the others laboratories. For this reason, in Fig. 10e only the curves obtained by UniPD are reported. The average exploitation ratio is equal to 43% for tests performed at uniPD and 30% for tests performed at UniSalento.

4.3.6. C-FRCM_6

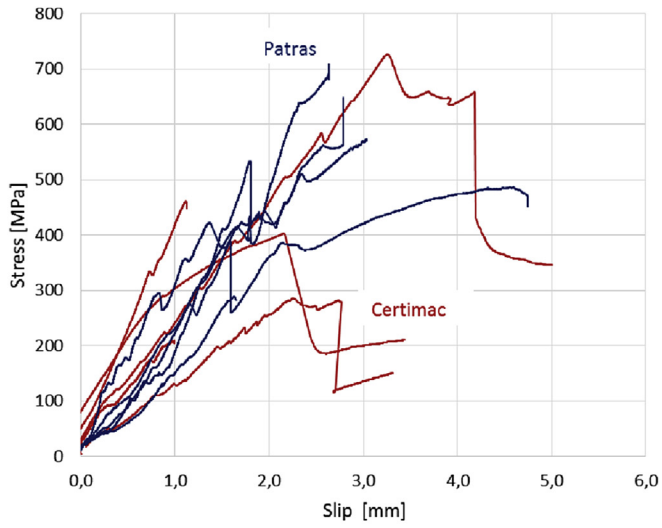
The tests performed at the University of Roma3 resulted in the failure (rupture) of one of the two yarns of the textile in the unbonded portion, followed by the rupture of the second yarn within the mortar matrix. The tests performed at the University of Patras resulted in fibers rupture within the bonded length, close to the loaded end. In one case, the detachment of a portion of the external matrix layer was observed. The average exploitation ratio varies between 70% and 85%.

4.4. Comment and comparison

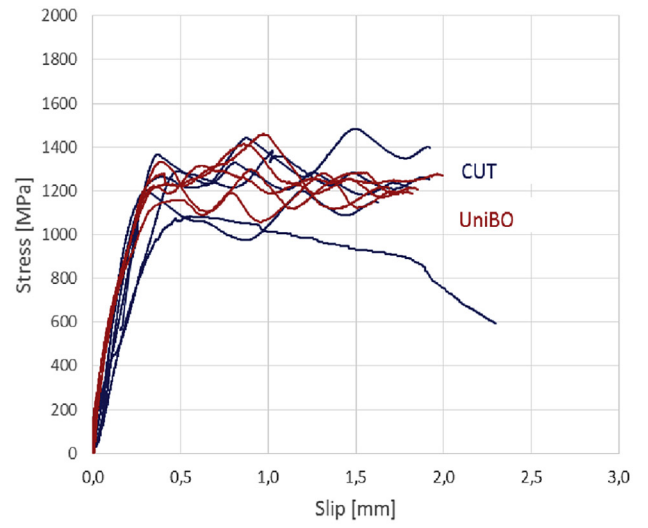
In this section an analysis of the main parameters that influence the experimental results and a comparison between the efficiency of the different analyzed systems are reported.

4.4.1. Test set-up and instrumentation

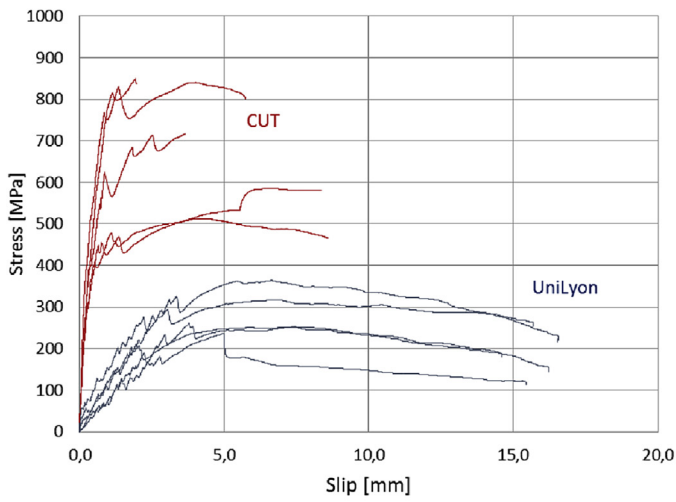
Due to the large variability of test parameters, materials involved and experimental results, it is not easy to present a reliable correlation between the test set-ups involved and the results obtained. The main differences are related to the clamping system of the textile and to the system used to guarantee the alignment between the reinforcement and the testing machine. The geometry of



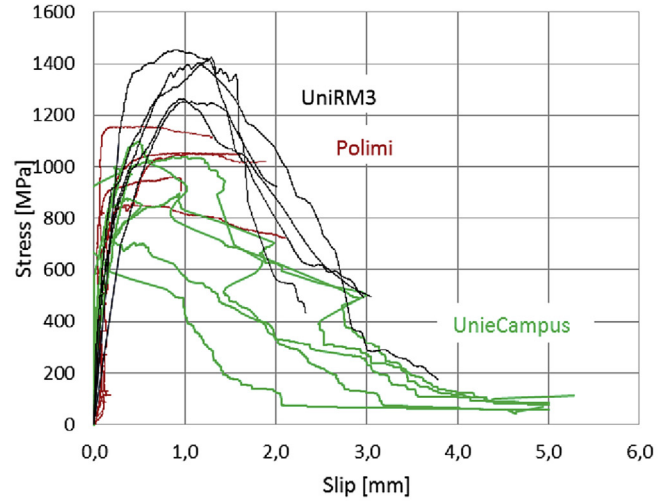
a



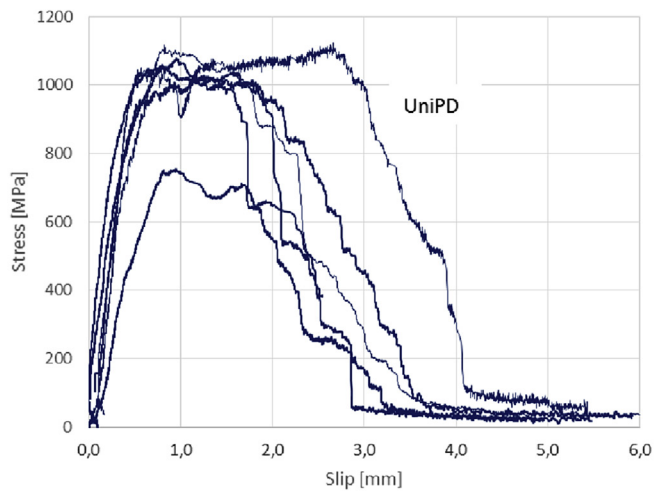
b



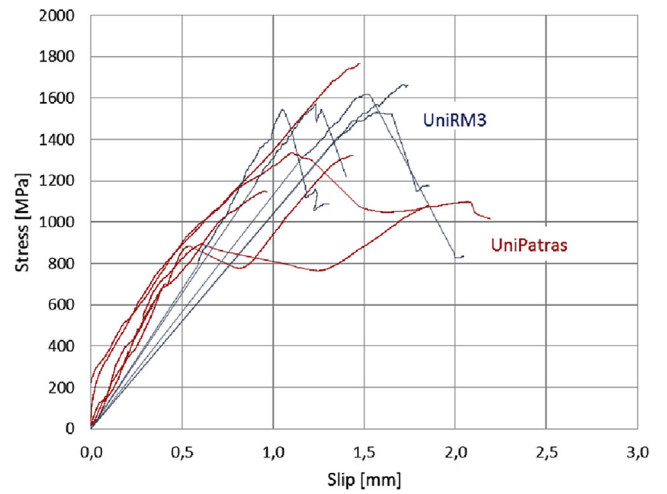
c



d



e



f

Fig. 10. Shear tests: stress-slip behaviour: a) C-FRCM_1; b) C-FRCM_2; c) C-FRCM_3; d) C-FRCM_4; e) C-FRCM_5; f) C-FRCM_6.

the specimen and the preparation phases can play a fundamental role. The width of the reinforcement, and in turn the number of yarns, could affect the load distribution between the yarns. A non-homogeneous stress distribution and the localization of the failure in some yarns was detected. Another problem could be the positioning of the textile between the internal and external mortar layers. If the external layer of the mortar is of low thickness, problems in the curing phase with the possibility of cracking phenomena (failure mode "E") could occur.

In many cases, a large scatter in the measurement of the slips between the textile and the matrix was observed. This could be attributed to the following reasons: different failure modes; non-homogeneous stress distribution among the yarns; different test rate, in particular in the post-peak phase; stress distribution between the filaments in the yarns, with the possible failure of the external filaments in the embedded area and a telescopic failure mode controlled only by the friction at the matrix/textile interface.

4.4.2. Comparison between different FRCM systems

Fig. 11 shows a comparison between average exploitation ratios obtained by the tests performed on different C-FRCM systems. The vertical bars show the standard deviation obtained by each laboratory. It is noted that the systems C-FRCM_4 and C-FRCM_6 present the best performance in terms of exploitation ratio. In these cases failure was caused by slippage between textile and matrix and by textile rupture, and an average exploitation ratio higher than 60% was reached. The C-FRCM_1 system shows a low exploitation ratio; the failure mode was characterized by cracking of the external layer of the mortar and by mortar spalling, probably due to the rigid link (stitch-bonded joints) between the yarns in the weft and warp directions. The C-FRCM_2 system shows an exploitation ratio equal to approximately 40% of the corresponding textile tensile strength. In this case, failure was mainly caused by poor bond properties between matrix and textile and to the mortar mechanical properties. Also, C-FRCM_3 system presents a low exploitation ratio with failure at mortar-textile interface and in few cases cracking of the external layer of mortar.

Fig. 12 shows a comparison between the pairs of stress-slip values for the tests performed on different C-FRCM materials. It can be noticed that a large part of the systems presents a stiffness that varies between 800 N/mm and 1200 N/mm. C-FRCM_1 and C-FRCM_3 systems present lower stiffness probably caused by a different failure mode characterized by slippage of the textile, poor FRCM-to-substrate bond capacity and cracking of the upper mortar layer.

5. Comparison between tensile and shear tests

The experimental work described shows large variability in the test results due to: different set-ups, influence of the operator in the preparation phase and test execution, and large differences between the tested systems. Despite these problems, tensile and shear tests are necessary in order to mechanically characterize FRCM materials. A comparison between these two tests is useful for the development of a qualification method that takes into account both the tensile and the bond properties of the material.

Comparison between tensile and shear tests is not an easy task because the boundary conditions and the stress developed are complete different. In particular, in the tensile test the entire cross-section is subjected to tensile stresses that are transferred from the matrix to the textile, as described in the previous paragraphs. The slippage phenomena between fabric and mortar are prevented by the clamping grips adopted in this work. After cracking of the mortar, slippage phenomena become complex as mortar penetrates in the yarns binding the outer filaments and leaving the inner

ones free to slip; this leads to the telescopic slippage of the filaments within the yarn [37]. In Ref. [38] a numerical simulation was presented to simulate the tensile tests on FRCM materials and compare possible constitutive models for the cementitious matrix. The stress distribution on different transversal cross-sections was shown and the influence of the tensile stress-strain relationship in tension adopted for the constitutive materials was investigated.

In the shear tests, the internal layer of mortar is bonded to the substrate and subjected to shear stresses and not directly to tensile ones; moreover, the load is directly applied to the textile. The numerical models described in Ref. [39] investigated the tangential stresses distribution in a shear test, assuming that all the deformability and the failure mechanism occurs in the FRCM system. The numerical models described showed, in agreement with intuition, that the stress states developed during a tensile and a shear tests are very different.

Despite these differences and the different mechanical meaning of the two tests presented in this paper, a comparison between the results obtained with these two tests could be useful to obtain a qualification method.

A standard procedure for product qualification and design should provide the mechanical parameters for the use of FRCM materials and combine simplicity and reliability. The safety requirements for an FRCM reinforcement system concern the tensile stress in the textile that must be lower than the tensile strength and lower than the stress inducing debonding of the reinforcement. In order to satisfy both these requirements [40] proposed a procedure based on the combination of the results of direct tensile and shear bond tests. The characteristic value of the ultimate axial stress obtained by shear tests is identified on the stress-strain response curve obtained by tensile tests together with the corresponding strain.

This procedure was applied to some of the test results previously described in order to highlight the possible problems due to the large variability in the behaviour of these systems.

In particular, in Fig. 13 the tests performed on C-FRCM_2 at the University of Bologna are analyzed. The shear tests resulted in a failure due to debonding at the textile-to-matrix interface whereas the peak stress varied between 1050 and 1300 MPa, which corresponds to the third phase of the stress-strain curve obtained by the tensile tests. The tensile tests failed under mode "B" and were characterized by a very small variability. By the intersection between the limit stress levels obtained by shear tests and the stress-strain curves of tensile tests, it is possible to obtain the limit strain and the corresponding secant elastic modulus [40]. For these tests the elastic modulus is equal to approximately 198 GPa.

Fig. 14 and Fig. 15 show the analysis of the experimental test results from C-FRCM_4 performed at Roma3 University and UnieCampus, respectively. In the first case, shear tests failed due to textile slippage and rupture near the loaded end of the bonded area. The limit stress varied between 1070 and 1400 MPa corresponding to the first and second phases of the stress-strain curve obtained by tensile tests, with a large variability. In this case, if the elastic modulus is computed considering the cross section area of the fibers, its value varies between 2525 GPa and 710 GPa. On the opposite, the tests performed at UnieCampus produced a limit stress value between 850 MPa and 1100 MPa, which correspond to the third phase of the stress-strain curve obtained by tensile tests. The tensile tests resulted in a failure mode "C" and a large variability. By the intersection between the limit stress level and the stress-strain curves of tensile tests it is possible to compute an elastic modulus that varies between 130 and 240 GPa.

These three examples show that this qualification method could give good results if the variability is low and if the intersection between the two tests results is localized in the third phase of the

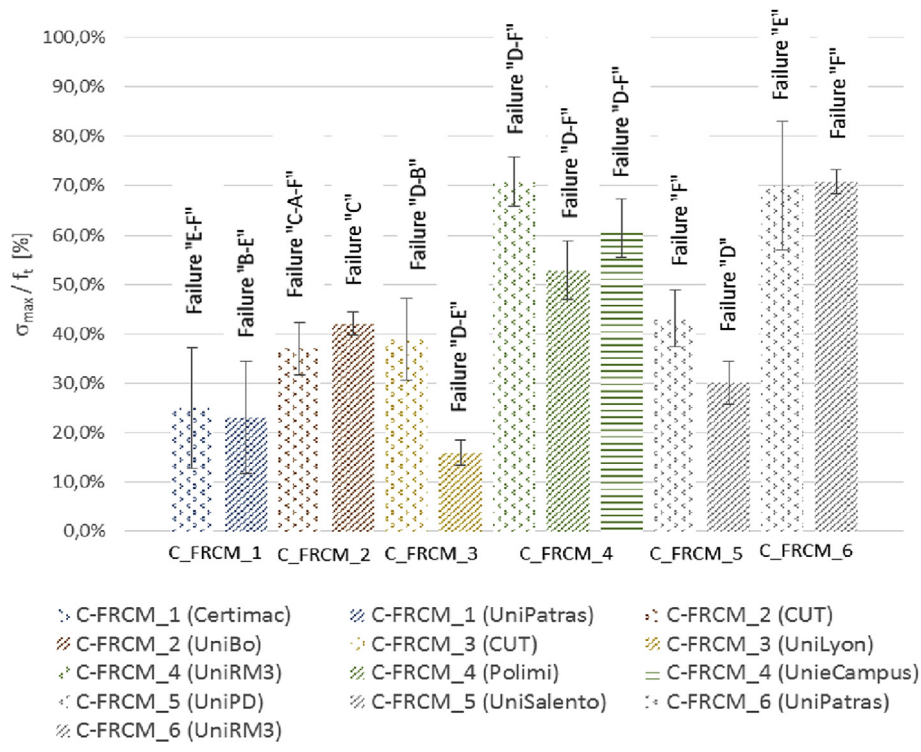


Fig. 11. Comparison between the exploitation ratios.

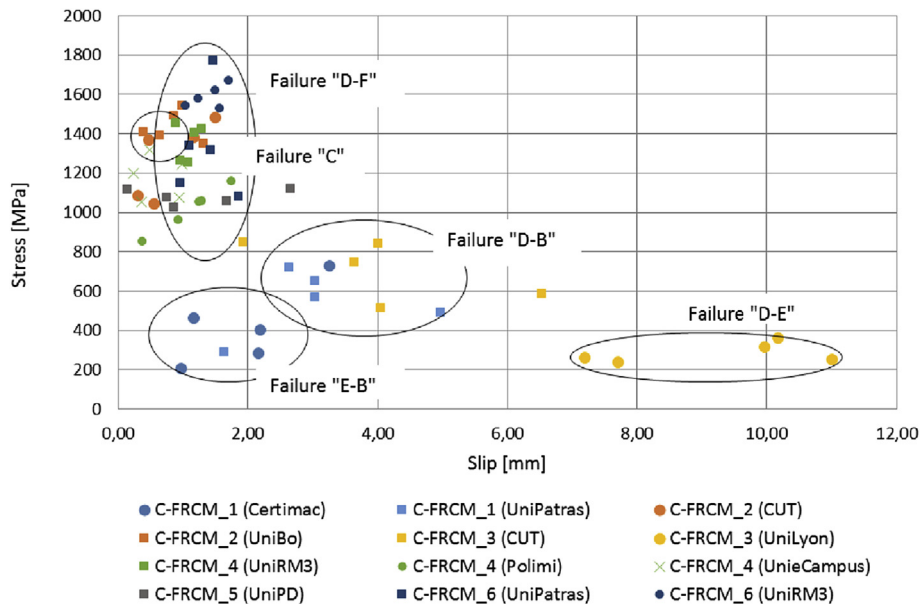


Fig. 12. Comparison between maximum stress and corresponding slip values.

stress-strain curve of tensile tests. Unfortunately, the results of this round robin experimental campaign showed that many factors could influence the tests and that the parameters that cause different responses between the different materials and test set-ups are many and difficult to be identified.

6. Conclusions

In this paper, the Round Robin experimental activities organized to study the characterization of fiber reinforced cementitious

matrix materials composed of carbon textiles and inorganic matrices is described. Ten laboratories from European universities and research centers were involved in the analysis of six different C-FRCM systems. The aim of this project was the study of a large number of FRCM materials and the involvement of many laboratories that used different instrumentation and set-ups.

The characterization of these materials involves both tensile and bond shear tests. The results of the experimental study and a discussion on the comparison between these two tests are also reported. The results gave information on several aspects, as

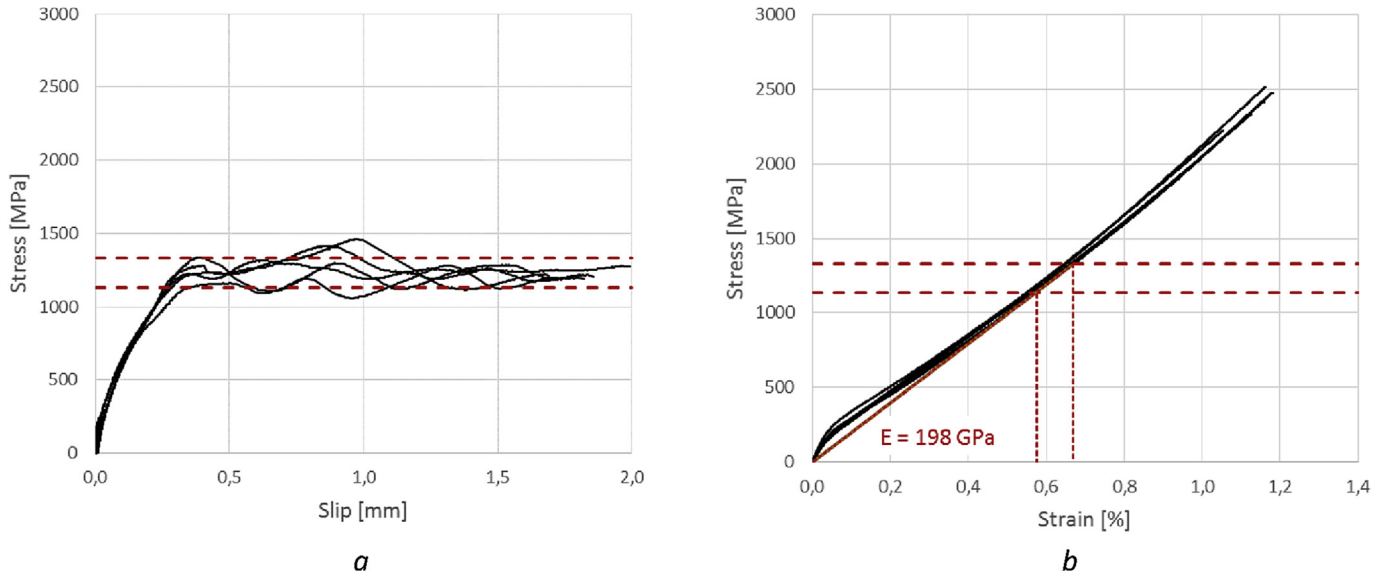


Fig. 13. C-FRCM_2—tests performed at UniBO. a) stress-slip behaviour of shear tests; b) stress-strain behaviour of tensile tests.

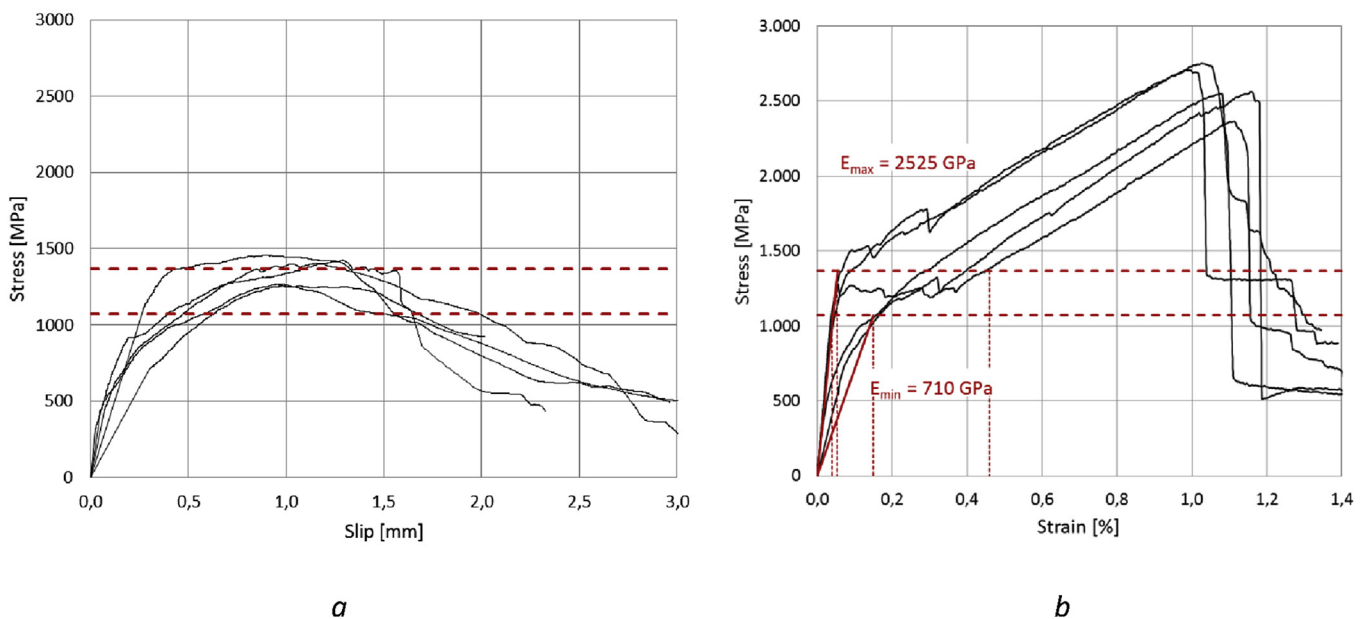


Fig. 14. C-FRCM_4—tests performed at UniRM3. a) stress-slip behaviour of shear tests; b) stress-strain behaviour of tensile tests.

described in the following.

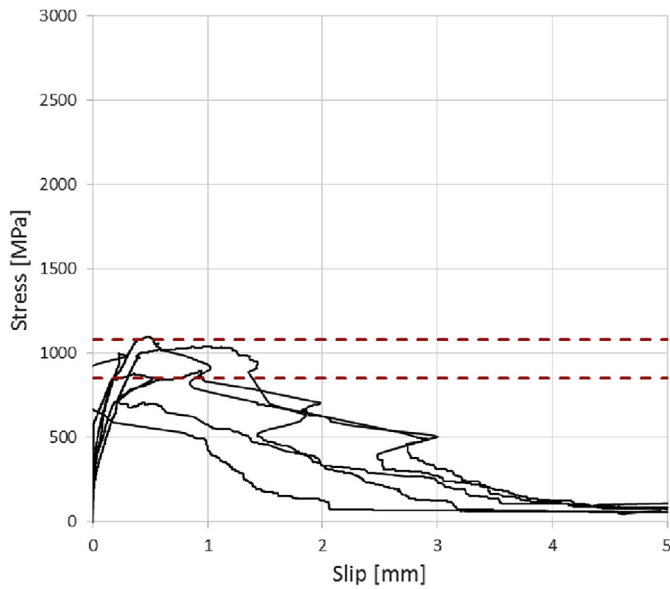
It is important to highlight the variability in the experimental results and the difficulty, in some cases, to compare the results of tests performed in different universities. This problem is due to the choice not to impose a unique specific testing procedure. This project allowed to evaluate the influence of the different test setups and samples characteristics, and could be an important contribution to individuate the more suitable test method.

6.1. Tensile tests

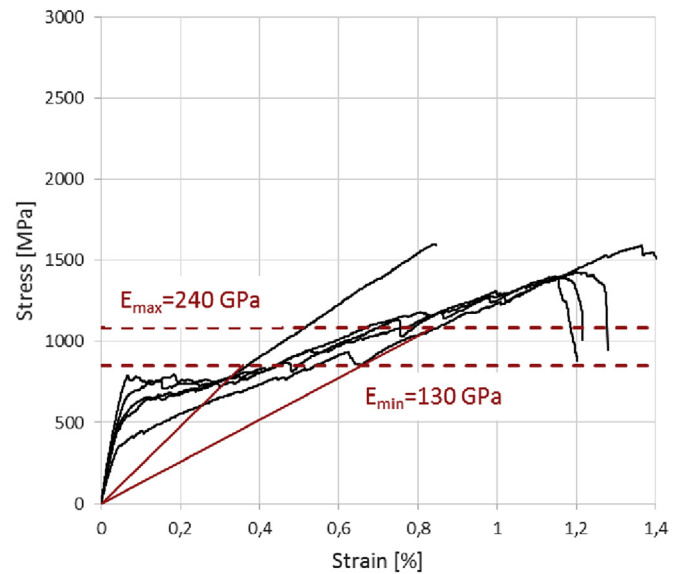
In general, the stress-strain curve obtained with a tensile test is characterized by three phases. In the initial elastic phase both matrix and textile are subjected to the load and the elastic modulus is very similar to the one of the matrix, due to the very low volumetric ratio of the textile. When the tensile strength of the mortar

is reached, the first cracks appear and the slope of the stress-strain curve decreases significantly. When crack saturation occurs, the only element subjected to the load is the textile, and both the slope of the stress-strain curve and the maximum attained stress are similar to those of the bare textile. Due to the large variability of the results, owed to the different clamping methods and to the different mechanical properties of the systems, not all results showed a tri-linear behaviour. In some cases the last phase is not present due to slippage phenomena.

Different failure modes were observed: the most common is cracking of the mortar associated with rupture of the textile, but in many cases also slippage of the textile at clamps was reported. The occurrence of this type of failure is related to the clamping system used and in particular to the pressure applied to the clamps. The most reliable clamping system involves reinforcement of the ends of the specimen with FRP materials and application of a pressure



a



b

Fig. 15. C-FRCM_4—tests performed at UnieCampus. a) stress-slip behaviour of shear tests; b) stress-strain behaviour of tensile tests.

sufficiently high to prevent both textile slippage and cracking of the matrix.

Different devices were used to measure the strain. The most important aspects that cause the variability in the strain measured at the end of each phase are the location of the first cracks with respect to the gauge length of the instrument, and the number of cracks included within the gauge length. Moreover, the failure mode largely influences the ultimate strain. If failure occurs due to the opening of a crack near the clamps and to the slippage of the textile, the strain measured by an external instrument with a gauge length lower than the length of the specimen (e.g. an extensometer) does not include this phenomenon.

Particular attention should be paid in the preparation and curing of the specimens. In particular, it should be checked that the textile is located at mid-thickness, the thickness of the mortar is constant, and no micro-cracks are present. These are the main aspects that caused the large variability that characterized the results of the tensile tests. Moreover, it is important to note that the variability is related to the inherent variability of the determination of the tensile strength of a mortar, and to the randomness of crack localization and evolution.

6.2. Shear bond tests

Different failure modes were highlighted, the most common being the slippage of the textile within the matrix and the rupture of the textile. In some cases, debonding at the matrix-textile interface and cracking of the external layer of mortar were also noted.

Specimens geometry and curing regimes largely affected the results. Large reinforcement widths can cause some problems in the alignment of the specimen and in the stress distribution. In addition, particular attention should be paid to the proper positioning of the textile with respect to the thickness of the mortar; textile misalignment could cause cracking of the external layer of mortar.

Large variability was highlighted in the measurement of the slippage between textile and matrix. Measuring the slippage, especially during the post-peak phase, could be quite difficult if the

failure mode includes fibers rupture.

Large differences were identified between different systems, in particular regarding the failure modes and the exploitation ratios. The main reason is the difference in the matrix-textile bond properties, which are influenced by the textile geometry, treatment of yarns (coating or impregnation) and the capability of the matrix to penetrate in the core filaments of the yarns (for not-coated yarns). Moreover, it is important to consider the degree of mechanical interlock that is achieved between the textile and the mortar. This parameter is influenced by the mesh size, the aggregate dimension of the mortar and by the rheological properties.

In the last part of the paper a comparison between tensile and shear experimental tests was reported. Due to the results variability and the problems previously described, it seems difficult to provide a unique method that allows to compare the mechanical properties and to classify the systems. The examples reported show that this qualification method is not robust and applicable to each material. In fact, the results are reasonable only if the intersection between the maximum stress reached with the shear test corresponds to the third phase of the stress-strain curve obtained by the tensile test.

The large experimental campaign described in this paper represents an important experimental database, supporting the drafting of guidelines for the characterization of FRCM materials and for the comparison of different systems. A deeper analysis should be performed to obtain information useful for design purposes.

Acknowledgements

The authors would like to thank the companies that supported the experimental project: SanMarco Terreal Italia S.r.l., Noale (Venice, Italy) for providing the bricks, and the following companies for providing the FRCM systems and for the support in the preparation of the samples: Ardea Progetti e Sistemi s.r.l. Basf, Fyfe Co. LLC, G&P Intech s.r.l, Ruredil S.p.A.

The authors would like to thank the researches that cooperated to the experimental campaign: Alberto Balsamo (University of Naples), Stefano De Santis (Roma Tre University), Aron Gabor (Laboratory of Composite Materials for Construction), Ivano

Iovinella (University of Naples), Piotr Krajewski (Cracow University of Technology), Arkadiusz Kwiecień (Cracow University of Technology), Marianovella Leone (University of Salento), Gian Piero Lignola (University of Naples), Claudio Mazzotti (University of Bologna), Mattia Morganti (Certimac), Andrea Prota (University of Naples), Francesca Roscini (Roma Tre University), Matteo Scafè (ENEA, Laboratori Tecnologie dei Materiali, Faenza), Lisa Sonzogni (Politecnico di Milano). The tests carried out by UnieCampus were performed in the laboratory of the Department of Structures for Engineering and Architecture of the University of Naples “Federico II” in cooperation with Francesco Fabbrocino.

References

- [1] Butler M, Mechtecherine V, Hempel S. Durability of textile reinforced concrete made with AR glass fibre: effect of matrix composition. *Mater Struct* 2010;43:1351–68.
- [2] Donnini J, De Caso y Basalo F, Corinaldesi V, Lancioni G, Nanni A. Fabric-reinforced cementitious matrix behavior at high-temperature: experimental and numerical results. *Compos Part B* 2017;108:108–21.
- [3] Nanni A. FRCM strengthening – a new tool in the concrete and masonry repair toolbox. *Concr Int Des Constr* 2012;34(4):43–9.
- [4] Corradi M, Borri A, Castori G, Sisti R. Shear strengthening of wall panels through jacketing with cement mortar reinforced by GFRP grids. *Compos B* 2014;64:33–42.
- [5] D’Ambrisi A, Focacci F, Luciano R, Alecci V, De Stefano M. Carbon-FRCM materials for structural upgrade of masonry arch road bridges. *Compos Part B* 2015;75:355–66.
- [6] Triantafyllou T, Papanicolaou C. Innovative applications of textile-based composites in strengthening and seismic retrofitting as well as in the prefabrication of new structures. *Adv Mater Res* 2013;3(1):26–41. 639–640.
- [7] Alecci V, Misseri G, Rovero L, Stipo G, De Stefano M, Feo L, et al. Experimental investigation on masonry arches strengthened with PBO-FRCM composite. *Compos Part B* 2016;100:228–39.
- [8] Marcari G, Basili M, Vestroni F. Experimental investigation of tuff masonry panels reinforced with surface bonded basalt textile-reinforced mortar. *Compos Part B* 2017;108:131–42.
- [9] AC 434. Proposed acceptance criteria for masonry and concrete strengthening using fiber-reinforced cementitious matrix (FRCM) composite system. 2013.
- [10] RILEM Technical Committee 232-TDT. Test methods and design of textile reinforced concrete. *Mater Struct* 2016;49:4923–7.
- [11] Hartig F, Haubler-Combe U, Schicktzan K. Influence of bond properties on the tensile behaviour of Textile Reinforced Concrete. *Cem Concr Compos* 2008;30:89–906.
- [12] Zhu D, Peled A, Mobasher B. Dynamic tensile testing of fabric-cement composites. *Constr Build Mater* 2011;25:385–95.
- [13] Contamine R, Si Larbi A, Hamelin P. Contribution to direct tensile testing of textile reinforced concrete (TRC) composites. *Material Sci Eng A* 2011;528:8589–98.
- [14] Arboleda D, Loreto G, De Luca A, Nanni A. Material characterization of fiber reinforced cementitious matrix (FRCM) composite laminates. *Proceedings for 10th International Symposium on Ferrocement and Thin Reinforced Cement Composite* 2012; Havana. 2012.
- [15] Papantoniou IC, Papanicolaou CG. Flexural behavior of one-way textile reinforced concrete (TRC)/reinforced concrete (RC) composite slabs. *Proceedings of the 15th European Conference on Composite Materials - ECCM15, Venice, Italy. 2012. p. 24–8. June 2012.*
- [16] Carozzi FG, Poggi C. Mechanical properties and debonding strength of Fabric Reinforced Cementitious Matrix (FRCM) systems for masonry strengthening. *Compos Part B* 2015;70:215–30.
- [17] De Santis S, de Felice G. Tensile behaviour of mortar-based composites for externally bonded reinforcement systems. *Compos Part B-Eng* 2015;68:401–13.
- [18] Hegger J, Will N, Bruckermann O, Voss S. Load bearing behavior and simulation of textile reinforced concrete. *Mater Struct (RILEM)* 2006;39(8):765–76.
- [19] Raupach M, Orlowsky J, Büttner T, Diltthey U, Schleser M. Epoxy-impregnated textiles in concrete – load bearing capacity and durability. *ICTRC* 2006:77–88.
- [20] Arboleda D, Carozzi FG, Nanni A, Poggi C. Testing procedures for the uniaxial tensile characterization of fabric-reinforced cementitious matrix composites. *J Compos Constr* 2016;20(3). ASCE. 04015063.
- [21] D’Antino T, Carloni C, Sneed LH, Pellegrino C. Matrix-fiber bond behavior in PBO FRCM composites: a fracture mechanics approach. *Eng Fract Mech* 2014;117:94–111.
- [22] de Felice G, De Santis S, Garmendia L, Ghiassi B, Larrinaga P, Lourenco PB, et al. Mortar-based systems for externally bonded strengthening of masonry. *Mater Struct* 2013;47(12):2021–37.
- [23] D’Ambrisi A, Feo L, Focacci F. Experimental and analytical investigation on bond between Carbon-FRCM materials and masonry. *Compos Part B* 2013;46:15–20.
- [24] Mazzotti C, Ferracuti B, Bellini A. Experimental bond tests on masonry panels strengthened by FRP. *Compos Part B* 2015;80:223–37.
- [25] De Santis S, de Felice G. Steel reinforced grout systems for the strengthening of masonry. *Compos Struct* 2015;134:533–48.
- [26] Valluzzi MR, et al. Round Robin Test for composite-to-brick shear bond characterization. *Material Struct* 2012;45(12):1761–91.
- [27] Ceroni F, Ferracuti B, Pecce M, Savoia M. Assessment of a bond strength model for FRP reinforcement externally bonded over masonry blocks. *Compos Part B* 2014;61:147–61.
- [28] Malena M, de Felice G. Debonding of composites on a curved masonry substrate: experimental results and analytical formulation. *Compos Struct* 2014;112:194–206.
- [29] Sneed LH, D’Antino T, Carloni C, Pellegrino C. A comparison of the bond behavior of PBO-FRCM composites determined with double-lap and single-lap shear tests. *Cem Concr Compos* 2015;64:37–48.
- [30] Leone M, Aiello MA, Balsamo A, Carozzi FG, Ceroni F, Corradi M, et al. Glass fabric reinforced cementitious matrix: tensile properties and bond performance on masonry substrate. *Compos Part B-Eng* 2017;127:196–214. <http://dx.doi.org/10.1016/j.compositesb.2017.06.028>.
- [31] Lignola GP, Caggegi C, Ceroni F, De Santis S, Krajewski P, Lourenço PB, et al. Performance assessment of basalt FRCM for retrofit applications on masonry. *Compos Part B-Eng* 2017;128:1–18. <http://dx.doi.org/10.1016/j.compositesb.2017.05.003>.
- [32] Caggegi C, Carozzi FG, De Santis S, Fabbrocino F, Focacci F, Hojdy L, et al. Experimental analysis on tensile and bond properties of PBO and Aramid fabric reinforced cementitious matrix for strengthening masonry structures. *Compos Part B-Eng* 2017;127:175–95. <http://dx.doi.org/10.1016/j.compositesb.2017.05.048>.
- [33] De Santis S, Ceroni F, de Felice G, Fagone M., Ghiassi B., Kwiecień A., et al. Round robin test on tensile and bond behavior of steel reinforced grout systems, *Compos part B*. DOI: 10.1016/j.compositesb.2017.03.052.
- [34] De Santis S., Carozzi F.G., De Felice G., Poggi C. Test methods for textile reinforced mortar, *Compos part B*. DOI: 10.1016/j.compositesb.2017.03.016.
- [35] D’Antino T, Catherine Papanicolaou CG. Mechanical characterization of textile reinforced inorganic-matrix composites. *Compos Part B-Eng* 2017;127:78–91. <http://dx.doi.org/10.1016/j.compositesb.2017.02.034>.
- [36] Carloni C, Verre S, Sneed LG, Ombres L. Loading rate effect on the debonding phenomenon in fibre reinforced cementitious matrix-concrete joints. *Compos Part B* 2017;108:301–14.
- [37] Banholzer B, Brockmann T, Brameshuber W. Material and bonding characteristics for dimensioning and modelling of textile reinforced concrete (TRC) elements. *Mater Struct* 2006;39:749–63.
- [38] Bertolesi E, Carozzi FG, Milani G, Poggi C. Numerical modeling of fabric reinforced cementitious matrix composites (FRCM) in tension. *Construction Build Mater* 2014;70:531–48.
- [39] Carozzi FG, Milani G, Poggi C. Mechanical properties and numerical modeling of Fabric Reinforced Cementitious Matrix (FRCM) systems for strengthening of masonry structures. *Compos Struct* 2014;107:711–25.
- [40] Ascione L, de Felice G, De Santis S. A qualification method for externally bonded Fibre Reinforced Cementitious Matrix (FRCM) strengthening systems. *Compos part B* 2015;78:497–506.